

The nematic-isotropic phase transition in linear fused hard-sphere chain fluids

K.M. Jaffer, S.B. Opps and D.E. Sullivan

Department of Physics and Guelph-Waterloo Program for Graduate Work in Physics

University of Guelph, Guelph, Ontario N1G 2W1, Canada

(November 20, 2016)

We present a modification of the generalized Flory dimer theory to investigate the nematic (N) to isotropic (I) phase transition in chain fluids. We focus on rigid linear fused hard-sphere (LFHS) chain molecules in this study. A generalized density functional theory is developed, which involves an angular weighting of the dimer reference fluid as suggested by decoupling theory, to accommodate nematic ordering in the system. A key ingredient of this theory is the calculation of the exact excluded volume for a pair of molecules in an arbitrary relative orientation, which extends the recent work by Williamson and Jackson for linear tangent hard-sphere chain molecules to the case of linear fused hard-sphere chains with arbitrary intramolecular bondlength. The present results for the N-I transition are compared with previous theories and with computer simulations. In comparison with previous studies, the results show much better agreement with simulations for both the coexistence densities and the nematic order parameter at the transition.

I. INTRODUCTION

The hard-sphere chain fluid has been widely studied in recent years as a model for polymeric and related liquids. Various theories have been applied to determine the thermodynamic properties of the model fluid, such as thermodynamic perturbation theory (TPT) [1–5], generalized Flory dimer theory (GFD) [6–8], scaled particle theory (SPT) [9–11] and various integral-equation theories [12–15]. Despite these studies, several limitations still characterize most theories for the hard-sphere chain fluid, including the independence of intramolecular structure on the surrounding medium in homogeneous fluids [2,3], the inability to account for liquid-crystalline ordering [2,3,8,15] and a general difficulty in formulating practical extensions of these theories to non-uniform systems. Several density-functional approaches [16–18] to the latter problem have been examined, but these have not overcome the other limitations mentioned above.

In this article, we investigate a systematic and straightforward density-functional method to begin resolving these limitations. We focus on a rather specific problem, namely to characterize the nematic-isotropic (N-I) phase transition in a fluid composed of *rigid* linear fused hard-sphere (LFHS) chain molecules. Several related works have examined this topic recently [8,11,15,19–21]. Mehta and Honnella [8] applied GFD theory to the LFHS fluid, but were restricted to examining the isotropic phase. This is also true of the integral-equation and SPT approaches studied in ref. [15], although some information about the N-I transition could be deduced from stability analysis of the isotropic phase. Refs. [11,19–21] studied the N-I transition in linear tangent hard-sphere (LTHS) chain fluids, using a density-functional approach based on the decoupling approximation introduced by Parsons [22] and Lee [23] for hard ellipsoids and hard spherocylinders. This approximation consists of a rescaling of the virial series originally used by Onsager [24] to account for the thermodynamic properties of a rigid-rod fluid. (Ref. [21] also describes an extension of the method to a fluid of semi-flexible chains.)

The formulation discussed here is very similar to that of refs. [19–21], but utilizes a concept closely related to that of the TPT and GFD theories, namely that the thermodynamic properties of the full chain fluid can be described by a judicious combination of those characterizing “reference” fluids composed of smaller sub-units, in particular monomers and dimers. Both formally and intuitively, this picture is well suited to describing fluids of *flexible* chain molecules [1–7]. A key ingredient of the present work, focusing on rigid rods, is that the excluded volume (and hence the second virial coefficient) for a pair of LFHS molecules in an arbitrary orientation can be written *exactly* as a linear combination of that for a pair of diatomic hard-sphere molecules and a pair of hard-sphere monomers. This property is based on a recent analysis of the orientation-dependent excluded volume for LTHS chains by Williamson and Jackson [25]. Here it is shown that the results of ref. [25] can be extended straightforwardly to linear *fused* hard-sphere chains of arbitrary intramolecular bondlength.

In the present article, the decoupling approximation is utilized in two stages. In the first stage, it is assumed that all higher-order virial coefficients scale (in terms of monomer and diatomic contributions) in the same way as the second virial coefficient. In the case of an isotropic fluid phase, the resulting approximation for thermodynamic properties is similar to that of GFD theory, but differs from the latter in reproducing the exact second virial coefficient. In the

second stage, the excess free energy of the reference dimer fluid is rescaled in terms of the free energy of the isotropic phase of this fluid. This rescaling incorporates the exact weighted angle-average of the pair excluded volume, as in the theories of refs. [19–21], and thus is able to account for nematic ordering, in contrast to the original GFD theory.

The theory is presented in Section II. Although the focus of this paper is on uniform phases of a rigid molecular fluid, Section II A begins with the more general case of a non-uniform fluid and extensions of the theory to semi-flexible molecules are indicated briefly. In Sections II B and II C, the theory is specialized to uniform phases of LFHS chains. Calculations and results are presented in Section III, including comparisons with available Monte Carlo data for the N-I transition of both LTHS and LFHS chains. It is found that the present theory overestimates the reduced pressure when compared with both simulations and previous theories. However, the present results for coexistence densities and the nematic order parameter at the transition are in excellent agreement with simulations and are more accurate than those predicted by other recent theories [11,19–21]. Section IV contains a summary and some conclusions.

II. THEORY

A. General

Here we consider a one-component fluid containing on average N molecules, each molecule (or “ n -mer”) consisting of a rigid linear chain of n atomic sites. The configuration of any such molecule labelled i is specified by the position \mathbf{r}_i of some arbitrarily chosen “center” of the molecule and by the orientational Euler angles $(\theta_i, \phi_i) \equiv \omega_i$ of the molecular chain axis relative to some space-fixed frame. We assume that the total intermolecular potential energy for N molecules is pairwise additive, and denote the pair potential between molecules i and j as $U_{(2)}(\mathbf{r}_i\omega_i, \mathbf{r}_j\omega_j)$.

The probability density for finding any molecule in a configuration $\mathbf{r}\omega$ is denoted $\rho(\mathbf{r}\omega)$, which is normalized such that

$$\int d\mathbf{r}d\omega \rho(\mathbf{r}\omega) = N. \quad (1)$$

The integration over molecular position is constrained to occur within the system volume V . In density-functional theory, the Helmholtz free energy F of the fluid is expressed as a functional of $\rho(\mathbf{r}\omega)$. A formally exact, generalized virial expansion of F in powers of $\rho(\mathbf{r}\omega)$ can be obtained by straightforward adaptation of that for monatomic fluids [26], and is given by

$$F = kT \int d\mathbf{r}d\omega \rho(\mathbf{r}\omega) [\ln(4\pi\rho(\mathbf{r}\omega)\Lambda) - 1 + \beta U_{ex}(\mathbf{r}\omega)] + \Delta F, \quad (2)$$

where T is temperature, k is Boltzmann’s constant, $\beta = (kT)^{-1}$, Λ is the thermal de Broglie “volume” of a molecule, and U_{ex} is any external potential field acting on the fluid. ΔF is the excess (over an ideal gas) Helmholtz free energy of the system, and is expressed by the virial series

$$\Delta F = kT \sum_{m=2}^{\infty} \frac{\hat{B}_m}{m-1}. \quad (3)$$

The generalized virial coefficients \hat{B}_m have a standard diagrammatic representation in terms of irreducible cluster integrals, where the vertices of the diagrams represent the product of functions $\rho(\mathbf{r}_1\omega_1), \rho(\mathbf{r}_2\omega_2), \dots, \rho(\mathbf{r}_m\omega_m)$ and the bonds denote the Mayer function

$$f(\mathbf{i}, \mathbf{j}) = e^{-\beta U_{(2)}(\mathbf{i}, \mathbf{j})} - 1. \quad (4)$$

For simplicity, the label \mathbf{i} is used to denote $\mathbf{r}_i\omega_i$. Thus,

$$\hat{B}_2 = -\frac{1}{2} \int d\mathbf{1}d\mathbf{2} \rho(\mathbf{1})\rho(\mathbf{2})f(\mathbf{1}, \mathbf{2}), \quad (5)$$

$$\hat{B}_3 = -\frac{1}{3} \int d\mathbf{1}d\mathbf{2}d\mathbf{3} \rho(\mathbf{1})\rho(\mathbf{2})\rho(\mathbf{3})f(\mathbf{1}, \mathbf{2})f(\mathbf{2}, \mathbf{3})f(\mathbf{3}, \mathbf{1}), \quad (6)$$

etc.

The preceding equations can be formally generalized to fluids of semi-flexible molecules on interpreting the symbol \mathbf{i} to include all internal coordinates of molecule i and replacing $U_{ex}(\mathbf{i})$ by the full one-body potential incorporating

internal bonding and flexibility constraints [27,28]. In the usual approach of density-functional theory, the distribution function $\rho(\mathbf{i})$ in the preceding expressions for F is considered to be an arbitrary function of the molecular configuration \mathbf{i} , while the equilibrium form of that distribution function is obtained by functional minimization of the corresponding grand canonical potential $\Omega = F - N\mu$, where μ is the chemical potential.

In the standard application of the decoupling approximation for the case of *uniform* fluids [22,23,29], the 2nd virial coefficient is treated exactly while the m th-order virial coefficient is approximated as

$$\hat{B}_m = \frac{\hat{B}_2}{\hat{B}_2^{ref}} \hat{B}_m^{ref}, \quad (7)$$

where \hat{B}_m^{ref} is the virial coefficient of an appropriate reference fluid. In previous works, the reference fluid has been chosen to be either a hard-sphere fluid [22,23] or the *isotropic* phase of the actual system being considered [19,20,29]. In either case, resummation of the virial series (3) then gives

$$\Delta F = \frac{\hat{B}_2}{\hat{B}_2^{ref}} \Delta F^{ref}. \quad (8)$$

(A generalization of this procedure for a non-uniform fluid of hard spherocylinders is described in ref. [30].) The GFD and TPT theories for fluids of chain molecules are based on a different choice of reference system, involving the decomposition of each molecule into its constituent monomers and constituent dimers. Although originally derived using quite different arguments, we can obtain the GFD theory using the present framework. First, at the level of the 2nd virial coefficient, we postulate that \hat{B}_2 can be written as

$$\hat{B}_2 = a_n^{(M)} \hat{B}_2^{(M)} + a_n^{(D)} \hat{B}_2^{(D)}, \quad (9)$$

where $a_n^{(M)}$ and $a_n^{(D)}$ are appropriate mixing parameters. Here, $\hat{B}_2^{(M)}$ is the generalized 2nd virial coefficient characterizing the fluid which results on decomposing each chain molecule into its constituent monomers, while $\hat{B}_2^{(D)}$ is the analogous quantity for the reference fluid of constituent dimers. Formally, the latter decomposition assumes that the number of monomers per chain n is even. However, we anticipate (as suggested by previous work on GFD and related theories [5,7,31]) that both the monomer and dimer reference fluids should be characterized by suitable *effective* values of the number of monomers n_M and number of dimers n_D , respectively. In accordance with the decoupling approximation, we assume that the mixing parameters $a_n^{(M)}$ and $a_n^{(D)}$ can be chosen so that (9) generates the exact \hat{B}_2 . This condition will be examined in subsection II B. If it is assumed that all higher-order virial coefficients \hat{B}_m scale in a similar manner, *i.e.*

$$\hat{B}_m = a_n^{(M)} \hat{B}_m^{(M)} + a_n^{(D)} \hat{B}_m^{(D)}, \quad (10)$$

then resummation of the series in (3) gives

$$\Delta F = a_n^{(M)} \Delta F^{(M)}[\rho_M(\mathbf{r})] + a_n^{(D)} \Delta F^{(D)}[\rho_D(\mathbf{r}\omega)]. \quad (11)$$

In this equation, $\rho_M(\mathbf{r})$ and $\rho_D(\mathbf{r}\omega)$ are the probability densities for monomers and dimers, respectively, while $\Delta F^{(M)}$ and $\Delta F^{(D)}$ are the corresponding excess free energies, which in general are functionals of the densities. For simplicity, we assume that the n -mer contains only one type of monomer and dimer sub-unit; the generalization to heteronuclear molecules is straightforward.

The standard GFD theory for isotropic, homonuclear hard-sphere chain fluids, as investigated previously in refs. [6–8], can be formulated from the theory presented here. In particular, GFD theory is obtained from eqs.(2), (11), and a *modified* form of the condition (9). In order to determine the parameters $a_n^{(M)}$ and $a_n^{(D)}$ in this case, (9) is applied with \hat{B}_2 and $\hat{B}_2^{(D)}$ *approximated* by the cross second virial coefficient between a monomer and the full n -mer and between a monomer and a dimer, respectively. An additional condition is then required to fix $a_n^{(M)}$ and $a_n^{(D)}$ uniquely, which turns out to be

$$n_M a_n^{(M)} + n_D a_n^{(D)} = 1. \quad (12)$$

This is consistent with the “initial conditions” that $a_n^{(M)} = 1$, $a_n^{(D)} = 0$ when $n = n_M = 1$ and $a_n^{(M)} = 0$, $a_n^{(D)} = 1$ when $n = n_M = 2n_D = 2$. With these approximations, one obtains

$$n_M a_n^{(M)} = -Y_n, \quad n_D a_n^{(D)} = 1 + Y_n, \quad (13)$$

where Y_n is the quantity defined in eq.(14) of Honnall and Hall [6].

In the next subsection, we shall specialize (9) and (11) to the case of a uniform fluid of rigid homonuclear hard-sphere chains. It will be shown that (9) can be satisfied *exactly* when using the exact values of \hat{B}_2 and $\hat{B}_2^{(D)}$ and with a unique choice for the parameters $a_n^{(M)}$ and $a_n^{(D)}$ depending only on the geometric properties of the molecules.

B. Application to LFHS Chains

Here we consider that the full chain molecule is a rigid rod composed of n identical hard-sphere atoms, each of diameter d , with adjacent atoms separated by bondlength l . In a *uniform* but possibly orientationally ordered fluid, the n -mer probability density takes the form

$$\rho(\mathbf{r}\omega) = \rho f(\omega), \quad (14)$$

where $\rho = N/V$ is the molecular number density and $f(\omega)$ is a normalized angular distribution function. The generalized second virial coefficient \hat{B}_2 defined by (5) becomes

$$\hat{B}_2 = -\frac{\rho^2 V}{2} \int d\mathbf{r}_{12} d\omega_1 d\omega_2 f(\omega_1) f(\omega_2) f(\mathbf{r}_{12}, \omega_1, \omega_2). \quad (15)$$

For hard-body interactions, this reduces to

$$\hat{B}_2 = \frac{\rho^2 V}{2} \int d\omega_1 d\omega_2 f(\omega_1) f(\omega_2) v_e^{(n)}(\theta_{12}), \quad (16)$$

where $v_e^{(n)}(\theta_{12})$ is the excluded volume between two rigid n -mers, which depends on the relative angle θ_{12} between their axes. Analogous expressions hold for the monomer and dimer virial coefficients, $\hat{B}_2^{(M)}$ and $\hat{B}_2^{(D)}$. In particular,

$$\hat{B}_2^{(D)} = \frac{\rho_D^2 V}{2} \int d\omega_1 d\omega_2 f(\omega_1) f(\omega_2) v_e^{(2)}(\theta_{12}), \quad (17)$$

where $\rho_D = n_D \rho$ is the number density of dimers and $v_e^{(2)}(\theta_{12})$ is the corresponding excluded volume. Note that for rigid linear rods, the same angular distribution function, $f(\omega)$, characterizes the full rod and any diatomic subunit of the rod. For the monomer fluid,

$$\hat{B}_2^{(M)} = \frac{\rho_M^2 V}{2} v_e^{(1)}, \quad (18)$$

where $\rho_M = n_M \rho$ is the monomer number density. The monomer excluded volume $v_e^{(1)}$, of course, has no angular dependence. Requiring that (9) holds exactly then implies the following relation between the excluded volumes, *independent of the angular distribution function and number densities*,

$$v_e^{(n)}(\theta_{12}) = a_n^{(M)} n_M^2 v_e^{(1)} + a_n^{(D)} n_D^2 v_e^{(2)}(\theta_{12}). \quad (19)$$

Using analytic results for the angle-dependent excluded volume between rigid n -mers first derived by Williamson and Jackson (WJ) [25], we shall show that (19) is indeed satisfied exactly for appropriate values of $a_n^{(M)}$ and $a_n^{(D)}$. The work of WJ was restricted to linear tangent hard-sphere chains, but it is straightforward to generalize their analysis to LFHS chains of arbitrary bondlength l . Details are contained in the appendix. The basic result is (see (A3))

$$v_e^{(n)}(\theta_{12}) = v_e^{(n)}(0) + (n-1)^2 v_c^{(2)}(\theta_{12}), \quad (20)$$

where $v_e^{(n)}(0)$ is the excluded volume for two parallel n -mers ($\theta_{12} = 0$), given by (A1) and (A2), and $v_c^{(2)}(\theta_{12})$ is the contribution from the so-called “central region” (in the terminology of WJ) of the overlap volume between two diatomic molecules. This is given by (A15) in the appendix. Note that, contrary to the remarks by WJ, the latter involves “compact and tractable” analytic formulae.

Before comparing (19) and (20), one rewriting of the former is required. As already noted, the “reference” monomer and dimer fluids may be characterized by “effective” values of the numbers n_M and n_D . Similarly, it may be allowed that the diameters and bondlengths of the reference particles differ from those of the original chain molecule. This

feature arises in GFD theory [7,31] due to the assumption that the volume fractions of the reference fluids should equal that of the original n -mer fluid, $\eta = \rho v_n$, where v_n is the n -mer molecular volume. Equivalently, this requires that $v_n = n_M v_1 = n_D v_2$, where v_1 and v_2 are the molecular volumes of the reference monomers and dimers, respectively [32]. The equality of the volume fractions of the reference fluids and n -mer fluid arises automatically in the case of tangent hard-sphere chains with $l = d$, and no adjustment of the number and sizes of reference particles is needed. This is no longer true when a chain of fused hard spheres ($l < d$) is decomposed into reference monomers and dimers [7,31]. Therefore, we suppose that the diameter of a reference monomer is denoted d_M , the diameter of a monomer in a reference dimer is denoted d_D , while the bondlength of the reference dimer is denoted l_D . It is these lengths which characterize the excluded volumes $v_e^{(1)}$ and $v_e^{(2)}(\theta_{12})$ in (19), whereas all terms in (20) for $v_e^{(n)}(\theta_{12})$ are characterized by the diameter d and bondlength l of the original n -mer. Hence, it is appropriate to rewrite (19) in terms of the original molecular dimensions. On dimensional grounds, as confirmed by the equations in the appendix, the dimer excluded volume scales as

$$v_e^{(2)}(\theta_{12}, d_D, l_D) = d_D^3 \Psi \left(\theta_{12}, \frac{l_D}{d_D} \right), \quad (21)$$

where the dependence of $v_e^{(2)}(\theta_{12})$ on molecular lengths has been indicated. Then (19) can be rewritten as

$$v_e^{(n)}(\theta_{12}) = a_n^{(M)} n_M^2 \left(\frac{d_M}{d} \right)^3 v_e^{(1)} + a_n^{(D)} n_D^2 \left(\frac{d_D}{d} \right)^3 v_e^{(2)}(\theta_{12}), \quad (22)$$

where $v_e^{(1)}$ and $v_e^{(2)}(\theta_{12})$ now refer to the *original* monomer and dimer inside the n -mer. (Note $v_e^{(1)} = 4\pi d^3/3$.) Comparing (20) and (22) now gives

$$n_D a_n^{(D)} = \left(\frac{d}{d_D} \right)^3 \frac{(n-1)^2}{n_D}, \quad (23)$$

and

$$\begin{aligned} n_M a_n^{(M)} &= \left(\frac{d}{d_M} \right)^3 \frac{[v_e^{(n)}(0) - (n-1)^2 v_e^{(2)}(0)]}{n_M v_e^{(1)}} \\ &= \left(\frac{d}{d_M} \right)^3 \frac{(n-2)}{n_M} [2(n-1) \left(1 - \frac{3}{4} \left(\frac{l}{d} \right) + \frac{1}{16} \left(\frac{l}{d} \right)^3 \right) + (2-3n)], \end{aligned} \quad (24)$$

where the second line in (24) follows from (A1) and (A2) in the appendix. Equations (23) and (24) have been written in terms of the combined parameters $n_M a_n^{(M)}$ and $n_D a_n^{(D)}$ because, as will be seen in the next subsection, only these combinations appear in the expressions for thermodynamic functions. As stated at the end of the previous subsection, $a_n^{(D)}$ and $a_n^{(M)}$ are seen to depend only on the geometric properties of the molecules.

Of several prescriptions introduced in GFD theory [7,31] to adjust the effective parameter values, our reliance on the scaling relation (21) restricts us to those which conserve the reduced bondlength, $l_D/d_D = l/d \equiv l^*$. These are the approaches analogous to the A, C, and AC versions of GFD theory [7]. However, it turns out that these methods all yield *identical* thermodynamic results in the present theory. This follows from the fact that, according to (23) and (24), $n_M a_n^{(M)}$ and $n_D a_n^{(D)}$ depend on the diameters and numbers (for fixed l^*) only through the combinations $n_M (d_M/d)^3$ and $n_D (d_D/d)^3$, respectively, the values of which are uniquely determined by the condition of equal volume fractions [32].

Let us briefly compare the present expressions for $a_n^{(D)}$ and $a_n^{(M)}$ in (23) and (24) with those given by GFD theory for LFHS chains. The latter were derived recently by Mehta and Honnella [8] using GFD-A theory, which corresponds to taking $d_M = d_D = d$ while the effective numbers of monomers n_M and dimers n_D are adjusted to conserve volume fraction. For this case, Mehta and Honnella [8] showed that the function Y_n in (13) has the value $(n-2)$ and thus (13) reduces to

$$n_M a_n^{(M)} = -(n-2) \quad , \quad n_D a_n^{(D)} = n-1 \quad (GFD - A) \quad (25)$$

independent of bondlength. For simplicity, we compare (25) with (23) and (24) in the case of tangent spheres, for which $n_M = n$ and $n_D = n/2$. Eqs.(23) and (24) then give

$$\begin{aligned} n_M a_n^{(M)} &= \frac{(n-2)(11-19n)}{(8n)} \rightarrow -\frac{19}{8}n \\ n_D a_n^{(D)} &= \frac{2(n-1)^2}{n} \rightarrow 2n, \end{aligned} \quad (26)$$

where we indicate the leading asymptotic dependence for large n . In this limit, the present parameters $n_M a_n^{(M)}$ and $n_D a_n^{(D)}$ have nearly double the magnitude of those given by GFD theory. This leads, via $a_n^{(D)}$, to a significantly stronger angular dependence of the excluded volume (19) than would be predicted by GFD theory. One notes that $a_n^{(M)}$ is negative for $n > 2$ according to both (25) and (26), and thus the non-ideal thermodynamic behavior of the fluid can be considered to involve a *subtraction* of the behavior of the monomer fluid from that of the dimer fluid. It can be shown [33] that the approximate factor of two difference between GFD and the present theory for the separate parameters $a_M a_n^{(M)}$ and $n_D a_n^{(D)}$ largely cancels out for the second virial coefficient in an isotropic phase, consistent with the findings of Mehta and Honnella [8]. By construction, the present theory yields exact values of \hat{B}_2 in both isotropic and nematic phases of LFHS chain fluids with arbitrary n .

C. Free Energy Minimization

The total Helmholtz free energy F for a uniform one-component LFHS chain fluid follows from (2), (11), and (14):

$$F = kT\rho V \int d\omega f(\omega) [\ln(4\pi\Lambda\rho f(\omega)) - 1] + a_n^{(M)} \Delta F^{(M)}(\rho_M) + a_n^{(D)} \Delta F^{(D)}(\rho_D; [f(\omega)]). \quad (27)$$

The notation in (27) for $\Delta F^{(M)}$ and $\Delta F^{(D)}$ is meant to indicate that the former is a function of the monomer number density ρ_M , while the latter is a function of ρ_D while being a *functional* of the angular distribution $f(\omega)$.

For the isotropic phase, we shall follow previous work on GFD theory and use the “exact” Carnahan-Starling [34] and Tildesley-Streett [35] equations of state to obtain $\Delta F^{(M)}$ and $\Delta F^{(D)}$:

$$\frac{\Delta F^{(M)}(\rho_M)}{V kT} = \rho_M \frac{\eta(4-3\eta)}{(1-\eta)^2} \equiv \rho_M a_{CS}(\eta), \quad (28)$$

$$\begin{aligned} \frac{\Delta F^{(D)}(\rho_D)}{V kT} &= \rho_D [H' \ln(1-\eta) + \frac{\eta}{2(1-\eta)^2} [2(F' + H') - (F' - G' + 3H')\eta]] \\ &\equiv \rho_D a_{TS}(\eta), \end{aligned} \quad (29)$$

where

$$\begin{aligned} F' &= F + 3 = 4 + 0.37836l^* + 1.07860(l^*)^3, \\ G' &= G - 3 = -2 + 1.30376l^* + 1.80010(l^*)^3, \\ H' &= H - 1 = 2.39803l^* + 0.35700(l^*)^3, \end{aligned} \quad (30)$$

(and where F , G , H denote the same quantities as defined by Tildesley and Streett [35]). As stated earlier, the volume fraction η is assumed to be the same for the n -mer, dimer, and monomer fluids. In a uniform nematic fluid, the excess monomer free energy is still given by (28). The simplest conceivable ansatz for $\Delta F^{(D)}(\rho_D; [f(\omega)])$ is that suggested by decoupling theory [22,23,29], namely

$$\Delta F^{(D)}(\rho_D; [f(\omega)]) = \Delta F^{(D)}(\rho_D) J[f(\omega)], \quad (31)$$

where J is given by

$$J[f(\omega)] = \frac{\int d\omega_1 d\omega_2 f(\omega_1) f(\omega_2) v_e^{(2)}(\theta_{12})}{\int d\omega_1 d\omega_2 v_e^{(2)}(\theta_{12}) / (4\pi)^2}. \quad (32)$$

From (17), the functional $J[f(\omega)]$ is equivalent to the ratio between the second virial coefficients of the nematic and isotropic dimer fluids.

A self-consistent equation determining the equilibrium form of the angular distribution function follows by functional minimization of F with respect to $f(\omega)$, subject to the normalization condition $\int d\omega f(\omega) = 1$. We obtain

$$f(\omega) = \frac{e(\omega)}{\int d\omega' e(\omega')}, \quad (33)$$

where

$$e(\omega_1) = \exp \left[-2n_D a_n^{(D)} a_{TS}(\eta) \frac{\int d\omega_2 f(\omega_2) v_e^{(2)}(\theta_{12})}{\int d\omega_1 d\omega_2 v_e^{(2)}(\theta_{12}) / (4\pi)^2} \right] \quad (34)$$

and we have used the fact that $\rho_D = n_D \rho$. The excluded volume $v_e^{(2)}(\theta_{12})$ in (32) and (34) is that for reference dimers of diameter d_D and bondlength l_D , but explicit factors of d_D^3 cancel in the ratio of integrals due to the scaling law (21) and only the reduced bondlength l^* is required in specifying those integrals.

For a given volume fraction η , the integral equation (33) is solved numerically by iteration as in ref. [29]. To evaluate the angular integrals involving $v_e^{(2)}(\theta_{12})$ in (34), we express the molecular orientation $\omega_i \equiv (\theta_i, \phi_i)$ in the director frame of reference, *i.e.*, with polar angle θ_i measured from the nematic director axis. Then $f(\omega_i) = f(\theta_i)$ is independent of the azimuthal angle ϕ_i . The angle θ_{12} between the two rod axes can be expressed as

$$\cos \theta_{12} = \sin \theta_1 \sin \theta_2 \cos \phi_2 + \cos \theta_1 \cos \theta_2, \quad (35)$$

(where we arbitrarily set $\phi_1 = 0$). Then

$$\int d\omega_2 f(\omega_2) v_e^{(2)}(\theta_{12}) = \int_0^\pi \sin \theta_2 d\theta_2 f(\theta_2) \bar{v}_e^{(2)}(\theta_1, \theta_2), \quad (36)$$

where

$$\bar{v}_e^{(2)}(\theta_1, \theta_2) = \int_0^{2\pi} d\phi_2 v_e^{(2)}(\theta_{12}). \quad (37)$$

Using the analytic formulae for $v_e^{(2)}(\theta_{12})$ from the appendix, the integrations over θ_2 and ϕ_2 in (36) and (37) are performed numerically by the trapezoid rule (for each pair of θ_1 and θ_2 , the integration over ϕ_2 has to be done only once). The variables $\cos \theta$ and ϕ are discretized on grids of typical stepsizes $\Delta(\cos \theta) = 0.005$ and $\Delta\phi = \pi/200$. Changing the frame of reference to relative orientations (θ_{12}, ϕ_{12}) could be applied to reduce the number of integration variables involved in the denominator of the exponential in (34), but for numerical consistency and with a view towards cancellation of errors, that integral is evaluated here in a manner analogous to (36) (noting that the integration $\int d\omega_1 / (4\pi)$ becomes redundant). Similar numerical integration techniques are used to evaluate $J[f(\omega)]$, the denominator of (33) and the order parameter S_2 defined by (44) in Section III A.

Once the numerical solution of (33) is obtained, the corresponding equilibrium thermodynamic potentials can be evaluated from the Helmholtz free energy given by eqs.(27)-(32). Substituting (33) into the logarithm of (27), one obtains

$$\frac{F}{kTV} = \rho \left[\ln \left(\frac{4\pi\rho\Lambda}{\int d\omega e(\omega)} \right) - 1 \right] + a_n^{(M)} \rho_M a_{CS}(\eta) - a_n^{(D)} \rho_D a_{TS}(\eta) J[f(\omega)]. \quad (38)$$

The chemical potential μ follows from

$$\mu = \left(\frac{\partial(F/V)}{\partial\rho} \right)_T. \quad (39)$$

Hence

$$\frac{\mu}{kT} = \ln \left[\frac{4\pi\rho\Lambda}{\int d\omega e(\omega)} \right] + n_M a_n^{(M)} \frac{\Delta\mu_M(\eta)}{kT} + n_D a_n^{(D)} J[f(\omega)] \left[\frac{\Delta\mu_D(\eta)}{kT} - 2a_{TS}(\eta) \right], \quad (40)$$

where $\Delta\mu_M$ and $\Delta\mu_D$ are the excess chemical potentials of the monomer and (isotropic) dimer fluids, respectively:

$$\begin{aligned} \frac{\Delta\mu_M(\eta)}{kT} &= a_{CS}(\eta) + \eta a'_{CS}(\eta), \\ \frac{\Delta\mu_D(\eta)}{kT} &= a_{TS}(\eta) + \eta a'_{TS}(\eta), \end{aligned} \quad (41)$$

where $a'(\eta) \equiv da(\eta)/d\eta$. Finally, the equilibrium pressure is obtained from $P = \rho\mu - F/V$, which gives

$$\frac{P}{kT} = \rho + \rho_M a_n^{(M)} \Delta Z_M(\eta) + \rho_D a_n^{(D)} J[f(\omega)] \Delta Z_D(\eta), \quad (42)$$

where ΔZ_M and ΔZ_D are the excess monomer and (isotropic) dimer compressibility factors, respectively, given by

$$\begin{aligned} \Delta Z_M(\eta) &= \eta a'_{CS}(\eta) = \frac{2\eta(2-\eta)}{(1-\eta)^3}, \\ \Delta Z_D(\eta) &= \eta a'_{TS}(\eta) = \frac{\eta(F' + G'\eta - H'\eta^2)}{(1-\eta)^3}. \end{aligned} \quad (43)$$

The isotropic limits of the preceding equations are obtained by setting $f(\omega) = 1/(4\pi)$. In this limit, $J[f(\omega)] = 1$. Coexistence between isotropic(I) and nematic(N) phases is then evaluated by solving the equations $P(\eta_I) = P(\eta_N)$ and $\mu(\eta_I) = \mu(\eta_N)$, which is done by a Newton-Raphson procedure.

III. RESULTS

A. LTHS Chains

We consider first the case of tangent hard-sphere n -mers, before examining n -mers with arbitrary bondlength. The primary limitation to our analysis of the theory is the lack of extensive simulation data available for comparison. Of the Monte Carlo studies which have examined hard-sphere chains, the majority have focused on semi-flexible systems of tangent chains. Several of these studies have dealt with the limit of infinite rigidity and therefore yield results which can be used here for comparison. In particular, the recent studies by Yethiraj and Fynewever [11,21] provide us with substantial analyses of the 8-mer and 20-mer LTHS chains. Williamson and Jackson [20] recently examined 7-mer LTHS chains and performed comparisons with theoretical treatments involving the exact excluded volume for the chains [25]. These studies will be the primary sources for comparisons with our results.

The conventional orientational order parameter S_2 is defined as

$$S_2 = \int P_2(\cos \theta) f(\omega) d\omega, \quad (44)$$

where P_2 is the second Legendre polynomial. This parameter has the limits of $S_2 = 0$ for an isotropic phase and $S_2 = 1$ for a perfectly aligned nematic phase. Figure 1 (a) and (b) show the order parameter S_2 as a function of volume fraction η for 8-mers and 20-mers, respectively. The Monte Carlo simulation data [11] is obtained using both constant-pressure (NPT) and constant-volume (NVT) methods, which are seen to be in very good agreement. This data is compared with the present theory and with the Parsons theory [22], as employed by Yethiraj and Fynewever [11,21] (using a simple *hard-sphere* reference fluid and incorporating the excluded volume derived by Williamson and Jackson [25]).

In general, the present theory is in very good agreement with the simulation data for the degree of ordering in each system. The order parameter at which the nematic phase first appears is of the order $S_2 > 0.5$. The degree of ordering continues to increase dramatically over an extremely short density range, until $S_2 \approx 0.8$, after which the value of the order parameter begins to level off. This general behavior is also evident in the Parsons theory, although the values obtained for S_2 and the coexistence densities are less accurate. For the 8-mer LTHS chain system, the values of the order parameter predicted by our theory are in excellent agreement with the values obtained by simulation. Our theoretical results for the 20-mers exhibit slightly lower values of S_2 in comparison with the simulations, although the amount of data available is much smaller in this case. The Parsons theory systematically underestimates the degree of ordering in the nematic phase, as is evidenced in Figs. 1(a) and (b).

In Figs. 2(a) and (b), the reduced pressure $P^* = Pv_n/kT$ is plotted as a function of volume fraction for the 8-mer and 20-mer LTHS chains, respectively. The simulation data clearly show the coexistence densities between the isotropic and nematic branches. The values for these densities as yielded by both theory and simulation are given in Table 1, along with the order parameter S_2 and P^* in the coexisting nematic phase. It is seen that the coexistence regions predicted by the present theory agree very well with simulation, although the reduced pressure at any density shows poor agreement. The present theory overestimates the value of P^* throughout the density range, a discrepancy which becomes more pronounced at higher densities. On the other hand, the Parsons theory predicts coexistence densities substantially higher than those observed in simulation, as well as a larger coexistence range, as is depicted

on both graphs. The Parsons theory underestimates the values of the reduced pressure as a function of density for both systems. Yethiraj and Fynewever [11] note that SPT treatments also underestimate the pressure for the 8-mer system, while overestimating it for larger molecules.

The 7-mer LTHS chain has been recently examined by Williamson and Jackson [WJ] [20] in light of the explicit calculation of the excluded volume for LTHS chains [25]. WJ performed Monte Carlo simulations for a system of $N = 576$ molecules. The results of the simulation were compared with several theories which were modified to incorporate the calculation of the exact excluded volume. In particular, WJ compare the simulation results with those obtained from a modified version of the Vega and Lago theory [19]. The original Vega and Lago theory is based on the form of the decoupling approximation in (7) and (8), where the reference fluid is the isotropic phase of the n -mer fluid. WJ modify the original Vega and Lago theory to incorporate their exact analytic calculation of the excluded volume into \hat{B}_2 , and obtain the isotropic phase free energy from TPT [1,36]. In Fig. 3, we compare the results for S_2 from the present theory with the Monte Carlo simulation data. As in Fig. 1, the present theory predicts the order parameter with excellent accuracy. The general behavior of S_2 is similar to the previous graphs. The comparison of reduced pressure versus volume fraction for the 7-mer system is made in Fig. 4. The modified Vega and Lago theory yields accurate pressures in comparison with simulation, but the predicted transition densities (evidenced by the plateau in the trace) are too low. This is also indicated in Table 1, which shows that the present theory yields coexistence densities lying within the ranges obtained through the simulations. The Vega-Lago theory also overestimates the value of S_2 in the nematic phase. However, as in Fig. 2, the values of reduced pressure given by the present theory clearly exceed the reported simulation data. This discrepancy appears to be systematic in the theory and will be discussed in Section IV. It should be noted here that the WJ simulation data predict a smectic phase to occur at volume fractions greater than 0.37.

The relationship between the length of molecules and the range of the coexistence region is shown in Fig. 5. The general trend is an increasing difference between the densities of the isotropic and nematic branches at coexistence as the number of monomers constituting the molecule increases. This trend is consistent with simulation, as is shown in this figure for 7-mers, 8-mers and 20-mers. The Parsons theory and various SPT treatments have yielded a similar trend [11], although these theories tend to overestimate the width of the coexistence region. In addition, the values of the coexistence densities obtained from these theories are in poor agreement with simulation, while the present theory provides a quantitatively accurate description of these densities.

B. LFHS Chains

Simulations of LFHS chains have been performed by Whittle and Masters [37] for the cases of 6-mers with a reduced bondlength of $l^* = 0.5$ and 8-mers with $l^* = 0.5$ and 0.6. These three systems were recently investigated by Mehta and Honnell [8] using GFD theory, comparing their results with the Whittle and Masters [37] simulation data and with a modification of TPT [1]. The GFD theory and the modified TPT are unable to treat ordering, and therefore are inappropriate at densities above the isotropic-nematic transition which was evidenced in the simulation of the 8-mer system with $l^* = 0.6$. In Fig. 6, we perform an analogous study of the three fluids, comparing the previous results [8] with those of the present theory. Figure 6(a) shows the reduced pressure as a function of volume fraction for the 6-mer LFHS chains with $l^* = 0.5$. There is no evidence of a nematic transition in the simulations, nor is there any indication through the theoretical treatments. The present theory and the modified TPT both overestimate the values of the reduced pressure, while the GFD theory appears to predict the reduced pressure to a fair degree of accuracy. This trend is also apparent in Figs. 6(b) and (c) for the 8-mer cases. In the latter plots, the present theory is seen to predict a stable nematic branch at sufficiently high volume fractions. The simulation data in Fig. 6(b) exhibit no such transition, and we are unaware of any other simulations which have been done for this system. It should be noted that the monomeric reference fluid does not exist as a stable fluid above $\eta \approx 0.494$ [8] and as such the theory is probably invalid at these high densities.

Figure 6(c) considers the 8-mer fluid with $l^* = 0.6$, a system which clearly exhibits nematic ordering. At first glance it appears that the present theory, while succeeding in predicting a stable nematic branch, predicts that it occurs at volume fractions much greater than the simulations indicate. However, it should be noted that although Whittle and Masters [37] report a nematic branching at $\eta \approx 0.33$, the order parameter was not found to be stable until much higher volume fractions, $\eta \geq 0.419$. The predictions of the present theory for transition properties are compared with the simulation results in Table 1. Once again, we see that there is good agreement for the value of the nematic order parameter S_2 .

It is of interest to examine the present theory in the “spherocylinder” limit, which is obtained in the limits $n \rightarrow \infty$, $l \rightarrow 0$, such that $L \equiv (n-1)l$ remains finite. As discussed in the appendix, our analytical result for the LFHS excluded volume reduces (as should be expected) to that for hard spherocylinders of cylinder length L in this limit. Figure 7

shows the nematic and isotropic coexistence volume fractions for LFHS n -mers as a function of n , for a fixed value of $L/d = 19$, in comparison with the values for spherocylinders obtained from the Lee theory [23] and from Monte Carlo calculations (using the Gibbs-Duhem integration procedure) by Bolhuis and Frenkel [38]. One sees that both the individual volume fractions and their differences increase slowly with n , and approach the asymptotic spherocylinder values reasonably well, although underestimating the coexistence width in the limit. In more detail, it can be shown that the present theory in the spherocylinder limit yields exactly the same angular distribution function $f(\omega)$, at a given volume fraction η , as in the Lee theory [23]. However, the free energy and pressure are actually predicted to *diverge* in this limit, which accounts for the narrower coexistence width found in Fig. 7.

IV. CONCLUDING REMARKS

In this paper, we have introduced two key modifications into the generalized Flory-dimer (GFD) theory to describe nematic behavior in hard-sphere chain fluids of arbitrary intramolecular bondlength. The first modification is the inclusion of the exact excluded volume and second virial coefficient for LFHS chain molecules, based on generalizing the earlier calculation of Williamson and Jackson [25]. This procedure results in mixing parameters for the reference monomer and dimer fluids which are dependent only on the geometric properties of the molecules (see (23) and (24)). A related feature is that the ansatz of equal volume fractions *uniquely* determines the values of the relevant combinations of the effective reference parameters n_D, d_D, n_M and d_M , in contrast to previous studies based on GFD and related theories [5,7,31]. The second modification of GFD theory, in order to account for the possibility of nematic ordering in the system, is the weighting of the excess dimer free energy by the ratio between the second virial coefficients of the nematic and isotropic dimer fluids (see (31) and (32)). This ansatz, suggested by decoupling theory, is dependent on the angular distribution function, which is determined self-consistently.

The present theory is found to be in excellent agreement with simulations of LTHS fluids in determining coexistence densities and the nematic order parameter as a function of density. As is seen clearly in Table 1 and Fig. 5, the transition densities for the 7-mer, 8-mer and 20-mer fluids predicted by the theory fall within the coexistence range found in simulations. In particular, the 7-mer system studied by Williamson and Jackson [20] shows much better agreement with the present theory than with the Vega and Lago [19] and the Parsons [22] theories for the coexistence densities as well as the nematic order parameter at the transition. The present theory is able to account for stable nematic branches in LFHS chains of sufficient length, for which theoretical work has been lacking up to now. The 8-mer with $l^* = 0.6$ simulated by Whittle and Masters [37] yielded transitions at lower densities than predicted by the present theory, although the simulated nematic branch did not become stable until densities similar to those predicted in our work. In addition, transitions between the isotropic and nematic phases are predicted by the present theory for several systems which have yet to be simulated (see Figs. 5 and 7). The agreement between the present theory and simulations is promising and it is hoped that further work will be encouraged.

For all systems studied, the present theory yields values for the pressure which exceed those given by available simulation data as well as previous theories. This discrepancy is not accounted for within this paper, and further work needs to be done to resolve the problem. It was noted in Section III B that the free energy and pressure given by the present theory actually diverge in the spherocylinder limit $n \rightarrow \infty, l \rightarrow 0$, with $(n-1)l \equiv L$ finite. This divergence can be traced to the incorrect limiting behavior of the Tildesley-Streett (TS) [35] dimer equation of state for small reduced bondlength l^* . The TS equation of state predicts that the reduced isotropic second virial coefficient (as well as higher virial coefficients) varies linearly with l^* (see (30)), in contrast with the correct leading-order variation proportional to $(l^*)^2$ (see (A17)). However, use of other dimer equations of state which do have the correct dependence for $l^* \rightarrow 0$, such as the “improved scale particle theory” of Boublik and Nezbeda [9], produces negligible differences from most of the results described in this paper, apart from those shown in Fig. 7 for $n \geq 40$.

Despite the mixed agreement of our results with those of available simulations, we believe that the approach described here has advantages over other current density functional theories of chain fluids [2,3,11,16–21], particularly for considering extensions of the theory to non-uniform fluids and ones containing semi-flexible molecules. In Section II A, we briefly indicated these generalizations of the theory, which we are currently investigating in more detail. Our approach retains the geometrically motivated spirit of the GFD and TPT theories in utilizing reference fluids composed of monomer and dimer subunits, whose properties can be readily determined. This contrasts with the form of the decoupling approximation used in refs. [19,20], requiring *a priori* information about the thermodynamics of the isotropic phase of the full system being considered, which may be either unavailable or computationally difficult to obtain in the more general cases. At the same time, the dimer reference fluid has the crucial property of involving orientational degrees of freedom. This feature corrects a limitation of previous density-functional approaches for non-uniform chain fluids [2,3,16–18] based on a purely monomeric reference fluid, which are unable to account for orientational ordering effects.

Acknowledgments. This work was supported by a research grant from the Natural Sciences and Engineering Research Council (Canada), and by a NATO Collaborative Research Grant. We are grateful to Drs. B.G. Nickel and C.G. Gray for their insightful comments.

APPENDIX : EXCLUDED VOLUME OF LFHS CHAINS

Williamson and Jackson (WJ) [25] recently derived an expression for the excluded volume between a pair of LTHS n -mers at an arbitrary relative orientation θ_{12} . Here we extend their analysis to LFHS n -mers of arbitrary bondlength.

The excluded volume for parallel orientation, $\theta_{12} = 0$, is a straightforward extension of the WJ result, and is described by a chain of $(2n - 1)$ overlapping spheres of radius d and volume $v_S = 4\pi d^3/3$ separated by the n -mer bondlength l . The volume is given by the relation

$$v_e^{(n)}(0) = (2n - 1)v_S - 2(n - 1)v_o. \quad (\text{A1})$$

The overlap volume between a pair of adjacent spheres, v_o , is dependent on the bondlength-to-diameter ratio l/d , and is given by

$$v_o = \frac{4\pi}{3}d^3 \left[1 - \frac{3}{4} \left(\frac{l}{d} \right) + \frac{1}{16} \left(\frac{l}{d} \right)^3 \right]. \quad (\text{A2})$$

For a pair of n -mer molecules in an arbitrary orientation θ_{12} , the excluded volume is represented diagrammatically as n^2 overlapping spheres of radius d whose centers lie on the corners of a rhombus (Fig. 8). The centers of adjacent spheres are separated by l and the rhombus has angle θ_{12} . We define the “central region” (in the terminology of WJ) as the parallelepiped based on the rhombus, taken to lie in the xy plane, and extending along the z axis to distances $\pm d$. As in WJ [25], it can be shown that the excluded volume outside the central region is equal to the excluded volume in the $\theta_{12} = 0$ orientation. Furthermore, one can show that the excluded volume contained within the central region for an n -mer is $(n - 1)^2$ times that of a dimer. The total excluded volume is thus given by

$$v_e^{(n)}(\theta_{12}) = v_e^{(n)}(0) + (n - 1)^2 v_c^{(2)}(\theta_{12}), \quad (\text{A3})$$

where $v_e^{(n)}(0)$ is given by (A1) and $v_c^{(2)}(\theta_{12})$ is the contribution from the central region to the excluded volume between two diatomic molecules.

Following WJ [25], it is convenient to evaluate $v_c^{(2)}(\theta_{12})$ by considering infinitely thin slices parallel to xy at varying heights z . Due to mirror symmetry in the xy plane, we need to examine only distances $0 \leq z \leq d$. There are three distinct ranges of z which must be considered. The outermost range of z is characterized by the absence of two-body overlaps between the circular cross-sections through the spheres. The total excluded area of a slice parallel to xy within this range is that of a circle,

$$A_c^I(z) = \pi(d^2 - z^2), \quad (\text{A4})$$

where z ranges from d to h_{II} , the height at which two-body overlaps begin to occur. The distance h_{II} is dependent on the magnitude of the angle between the molecules, θ_{12} . For large enough θ_{12} ($\pi/3 \leq \theta_{12} \leq \pi/2$), overlap between the circular cross-sections first occurs for adjacent pairs of spheres. At this height, the radius of a circular cross-section is $r = l/2$, and the corresponding value of $z = h_{II}$ is:

$$h_{II}^{(1)} = \sqrt{d^2 - (l/2)^2}. \quad (\text{A5})$$

For smaller θ_{12} ($0 \leq \theta_{12} \leq \pi/3$), the first two-body overlaps occur between opposing spheres (Fig. 9). This height is given by the relation

$$h_{II}^{(2)} = \sqrt{d^2 - l^2 \sin^2(\theta_{12}/2)}. \quad (\text{A6})$$

For both angular cases evaluated above, the region of two-body overlaps extends until $z = h_{III}$, at which height the circular cross-sections through the spheres begin overlapping in a three-body configuration. The value for this height is given by

$$h_{III} = \sqrt{d^2 - \left(\frac{l}{2 \cos(\theta_{12}/2)} \right)^2}. \quad (\text{A7})$$

Throughout the range $h_{III} < z < d$, the total excluded area of a parallel slice can be expressed as

$$A_c^{II}(z) = A_c^I(z) - A_o(z) \quad (\text{A8})$$

where $A_c^I(z)$ is given by (A4) while $A_o(z)$ is the total two-body overlap area between the circles at height z . This overlap area has distinct contributions depending on whether the overlapping spheres are adjacent or opposite from each other (Fig. 9), and is given by

$$A_o(z) = 2a_o(l, z) + a_o(\hat{l}, z), \quad (\text{A9})$$

where $\hat{l} = 2l \sin(\theta_{12}/2)$. Here, $a_o(l', z)$ is the area of overlap between a pair of circles of radius r , separated by l' , given by

$$a_o(l', z) = 2 \left[r^2 \cos^{-1} \left(\frac{l'}{2r} \right) - \left(\frac{l'}{2} \right) \left(r^2 - \frac{l'^2}{4} \right)^{\frac{1}{2}} \right], \quad (\text{A10})$$

keeping in mind that $r = \sqrt{d^2 - z^2}$. The relation (A10) differs from equation (7) of WJ by a factor of 2 because WJ calculate only half of the overlap area. Remembering that the contributions of the two types of overlap begin at different values of z , the total contribution to the central excluded volume from regions I and II is

$$\begin{aligned} v_c^{I,II}(\theta_{12}) &= 2 \int_{h_{III}}^d dz A_c^{II}(z) \\ &= 2\pi \left[d^2 (d - h_{III}) - \frac{1}{3} (d^3 - h_{III}^3) \right] \\ &\quad - 4 \int_{h_{III}}^{h_{II}^{(1)}} dz a_o(l, z) - 2 \int_{h_{III}}^{h_{II}^{(2)}} dz a_o(\hat{l}, z) \end{aligned} \quad (\text{A11})$$

where the additional factor of 2 in (A11) is due to mirror symmetry.

The integrals involving a'_o s are quoted by WJ as being “intractable”, but we have derived a compact and tractable form for the indefinite integral:

$$\begin{aligned} \int dz' a_o(l', z') &= 2 (d^2 z - z^3/3) \cos^{-1} \left(\frac{l'/2}{\sqrt{d^2 - z^2}} \right) - \frac{2}{3} l' z \left[d^2 - z^2 - (l'/2)^2 \right]^{1/2} \\ &\quad - l' \left[d^2 - \frac{1}{3} (l'/2)^2 \right] \sin^{-1} \left(\frac{z}{\sqrt{d^2 - (l'/2)^2}} \right) \\ &\quad + \frac{4}{3} d^3 \tan^{-1} \left[\frac{l' z / (2d)}{\left[d^2 - z^2 - (l'/2)^2 \right]^{1/2}} \right]. \end{aligned} \quad (\text{A12})$$

One can verify that the z-derivative of the right-hand side of (A12) equals $a_o(l', z)$.

The innermost part of the central region is defined by $z \leq h_{III}$, where three-body overlaps occur. The whole volume of this region is excluded, and thus its contribution from this region to $v_c^{(2)}$ is equal to

$$v_c^{III}(\theta_{12}) = 2l^2 d \left[\sin^2 \theta_{12} - \left(\frac{l}{d} \right)^2 \sin^2(\theta_{12}/2) \right]^{1/2}. \quad (\text{A13})$$

The total excluded volume of the central region is then

$$v_c^{(2)}(\theta_{12}) = v_c^{I,II}(\theta_{12}) + v_c^{III}(\theta_{12}), \quad (\text{A14})$$

where the various contributions are given by (A11) to (A13) for $\theta_{12} \leq \pi/2$. Due to chain inversion symmetry, the excluded volume for $\theta_{12} > \pi/2$ is given by $v_c^{(2)}(\theta_{12}) = v_c^{(2)}(\pi - \theta_{12})$. Substituting the expressions for $h_{II}^{(1)}, h_{II}^{(2)}$ and

h_{III} from (A5), (A6) and (A7) into (A11) and (A12), and applying several trigonometric identities (most importantly the relation $\tan^{-1}(A) - \tan^{-1}(B) = \tan^{-1}[(A - B)/(1 + AB)]$), we are able to reduce the result for $v_c^{(2)}(\theta_{12})$ to the following compact form:

$$\begin{aligned} v_c^{(2)}(\theta_{12}) = & \left(\frac{2}{3} l^2 d \right) \sin(\theta_{12}/2) S(\theta_{12}) \\ & + 4l \left[d^2 - \frac{1}{3} \left(\frac{l}{2} \right)^2 \right] \tan^{-1} \left[\frac{l \sin(\theta_{12}/2)}{d S(\theta_{12})} \right] \\ & + 4l \sin(\theta_{12}/2) \left[d^2 - \frac{l^2}{3} \sin^2(\theta_{12}/2) \right] \tan^{-1} \left[\frac{l \cos(\theta_{12})}{d S(\theta_{12})} \right] \\ & - \left(\frac{8}{3} d^3 \right) \tan^{-1} \left[\frac{l^2 \sin(\theta_{12}/2) S(\theta_{12})}{4d^2 - l^2 (1 + 2 \sin^2(\theta_{12}/2))} \right], \end{aligned} \quad (\text{A15a})$$

where

$$S(\theta_{12}) = \left[4 \cos^2(\theta_{12}/2) - \frac{l^2}{d^2} \right]^{1/2}. \quad (\text{A15b})$$

It can be verified that the preceding result for the angle-dependent excluded volume of LFHS n -mers reduces to that for hard spherocylinders in the limit that $n \rightarrow \infty$, $l \rightarrow 0$, and $L \equiv (n-1)l$ remains finite, where L is identified with the cylinder length. In this limit, (A1) and (A2) give

$$v_e^{(n)}(0) \rightarrow \frac{4\pi d^3}{3} \left(1 + \frac{3}{2} \frac{L}{d} \right) \equiv 8v_{SC}, \quad (\text{A16})$$

where v_{SC} is the spherocylinder molecular volume. From (A15a,b), one finds readily that

$$v_c^{(2)}(\theta_{12}) = 2l^2 d \sin \theta_{12} + O(l^4). \quad (\text{A17})$$

The total excluded volume (A3) then becomes

$$v_e^{(n)}(\theta_{12}) \rightarrow 8v_{SC} + 2L^2 d \sin \theta_{12}, \quad (\text{A18})$$

which agrees with the result derived for hard spherocylinders [23,24].

TABLE 1. Coexistence results from simulation and theory.

LFHS Chain	Source	$\eta(iso)$	$\eta(nem)$	$S_2(nem)$	P^*
7-mer, $l^* = 1.0$	Present theory	0.2903	0.2989	0.6491	4.94
	MC-NPT data [20]	0.266-0.303	0.285-0.312	0.64-0.66	3.15-3.78
	Vega-Lago theory [20]	0.255	0.273	≈ 0.7	2.78
	Parsons theory [20]	0.303	0.319	N/A	3.12
8-mer, $l^* = 1.0$	Present theory	0.2601	0.2689	0.6538	3.95
	MC-NPT data [11]	0.257	0.271	≈ 0.7	2.65
	Parsons theory [11,21]	0.280	0.305	≈ 0.7	2.6
20-mer, $l^* = 1.0$	Present theory	0.1158	0.1243	0.6947	0.97
	MC-NPT data [11]	0.105	0.120	≈ 0.7	0.62
	Parsons theory [11,21]	0.115	0.140	≈ 0.75	0.69
8-mer, $l^* = 0.5$	Present theory	0.4687	0.4768	0.6168	13.1
8-mer, $l^* = 0.6$	Present theory	0.4167	0.4251	0.6224	9.8
	MC-NPT data [37]		No transition found	0.624	5.7

FIG. 1. Variation of order parameter S_2 with volume fraction η , comparing present theory with the Parsons theory and Monte Carlo data[11,21], for (a)8-mer LTHS chains, and (b)20-mer LTHS chains.

FIG. 2. Variation of the reduced pressure with volume fraction η , comparing present theory with the Parsons theory and Monte Carlo data[11,21], for (a)8-mer LTHS chains, and (b)20-mer LTHS chains.

FIG. 3. Order parameter S_2 vs. volume fraction η for LTHS 7-mers, comparing present theory with Monte Carlo data[20].

FIG. 4. Reduced pressure for LTHS 7-mers as a function of volume fraction η , comparing present theory with Monte Carlo data and the modified Vega and Lago theory from Ref.[20].

FIG. 5. Comparison of volume fractions of the isotropic and nematic phases at coexistence for LTHS n -mers, as a function of the number of monomers n , between the present theory and Monte Carlo simulation data.

FIG. 6. Comparison of the reduced pressure between this work, the Mehta and Honnall GFD theory and the modified TPT in Ref.[8], and Monte Carlo simulations[37] for (a)LFHS 6-mers with bondlength to diameter ratio $l^* = 0.5$, (b)LFHS 8-mers, $l^* = 0.5$, and (c)LFHS 8-mers, $l^* = 0.6$.

FIG. 7. Volume fractions of the isotropic and nematic phases at coexistence as a function of number of monomers n for LFHS chains of constant length with $L/d = 19$. The spherocylinder limits are given by the Lee theory[23] and by the Monte Carlo simulation results of Bolhuis and Frenkel[38].

FIG. 8. Diagrammatic representation of the excluded volume for $n = 2$. The slice is taken through the $z = 0$ plane, where the radius of each circle is the monomer diameter, d .

FIG. 9. Second case for two-body overlap, when $0 < \theta_{12} < \pi/3$.

[1] M.S. Wertheim, *J. Chem. Phys.* **87**, 7323 (1987).

[2] E. Kierlik and M.L. Rosinberg, *J. Chem. Phys.* **97**, 9222 (1992).

[3] E. Kierlik and M.L. Rosinberg, *J. Chem. Phys.* **99**, 3950 (1993).

[4] J. Chang and S.I. Sandler, *Chem. Eng. Sci.* **49**, 2777 (1994).

[5] Y. Zhou, C.K. Hall and G. Stell, *J. Chem. Phys.* **103**, 2688 (1995).

[6] K.G. Honnell and C.K. Hall, *J. Chem. Phys.* **90**, 1841 (1989).

[7] L.A. Costa, Y. Zhou, C.K. Hall and S. Carra, *J. Chem. Phys.* **102**, 6212 (1995).

[8] S.D. Mehta and K.G. Honnell, *J. Phys. Chem.* **100**, 10408 (1996).

[9] T. Boublik and I. Nezbeda, *Chem. Phys. Lett.* **46**, 315 (1977);
T. Boublik, *Mol. Phys.* **44**, 1369 (1981).

[10] T. Boublik, *Mol. Phys.* **68**, 191 (1989).

[11] A. Yethiraj and H. Fynewever, *Mol. Phys.* **93**, 693 (1998).

[12] J.G. Curro and K.S. Schweizer, *Macromolecules* **20**, 1928 (1987).

[13] K.S. Schweizer and J.G. Curro, *Macromolecules* **21**, 3070,3082 (1988).

[14] Y.C. Chiew, *Mol. Phys.* **70**, 129 (1990).

[15] A. Chamoux and A. Perera, *Mol. Phys.* **93**, 649 (1998).

[16] S. Sen, J.M. Cohen, J.D. McCoy and J.G. Curro, *J. Chem. Phys.* **101**, 9010 (1994).

[17] C.E. Woodward and A. Yethiraj, *J. Chem. Phys.* **100**, 3181 (1994).

[18] A. Yethiraj and C.E. Woodward, *J. Chem. Phys.* **102**, 5499 (1995).

[19] C. Vega and S. Lago, *J. Chem. Phys.* **100**, 6727 (1994).

[20] D.C. Williamson and G. Jackson, *J. Chem. Phys.* **108**, 10294 (1998).

[21] H. Fynewever and A. Yethiraj, *J. Chem. Phys.* **108**, 1636 (1998).

[22] J.D. Parsons, *Phys. Rev. A* **19**, 1225 (1979).

[23] S.D. Lee, *J. Chem. Phys.* **87**, 4972 (1987).

[24] L. Onsager, *Ann. NY Acad. Sci.* **51**, 627 (1949).

[25] D.C. Williamson and G. Jackson, *Mol. Phys.* **86**, 819 (1995).

[26] G. Stell, in *The Equilibrium Theory of Classical Fluids*. H.L. Frisch and J.L. Lebowitz, eds. (Benjamin, New York, 1964).

[27] D. Chandler and L.R. Pratt, *J. Chem. Phys.* **65**, 2925 (1976).

[28] L.R. Pratt and D. Chandler, *J. Chem. Phys.* **66**, 147 (1977).

[29] P. Padilla and E. Velasco, *J. Chem. Phys.* **106**, 10299 (1997).

[30] A.M. Somoza and P. Tarazona, *J. Chem. Phys.* **91**, 517 (1989).

[31] A. Yethiraj, J.G. Curro, K.S. Schweizer and J.D. McCoy, *J. Chem. Phys.* **98**, 1635 (1993).

[32] Expressions for the molecular and reference volumes, v_n , v_1 and v_2 , are: $v_n = \frac{\pi d^3}{6} [1 + (n-1) (\frac{3}{2}l^* - \frac{1}{2}(l^*)^3)]$, $v_1 = \frac{\pi}{6} d_M^3$
and $v_2 = \frac{\pi d_P^3}{6} [1 + \frac{3}{2}l^* - \frac{1}{2}(l^*)^3]$.

[33] K.M. Jaffer, M.Sc. Thesis. University of Guelph, (1999).

[34] N.F. Carnahan and K.E. Starling, *J. Chem. Phys.* **51**, 635 (1969).

[35] D.J. Tildesley and W.B. Streett, *Mol. Phys.* **41**, 85 (1980).

[36] W.G. Chapman, G. Jackson and K. Gubbins, *Mol. Phys.* **65**, 1057 (1988).

[37] M. Whittle and A.J. Masters, *Mol. Phys.* **72**, 247 (1991).

[38] P. Bolhuis and D. Frenkel, *J. Chem. Phys.* **106**, 666 (1997).

Figure 1(a). K.M. Jaffer: J. Chem. Phys.

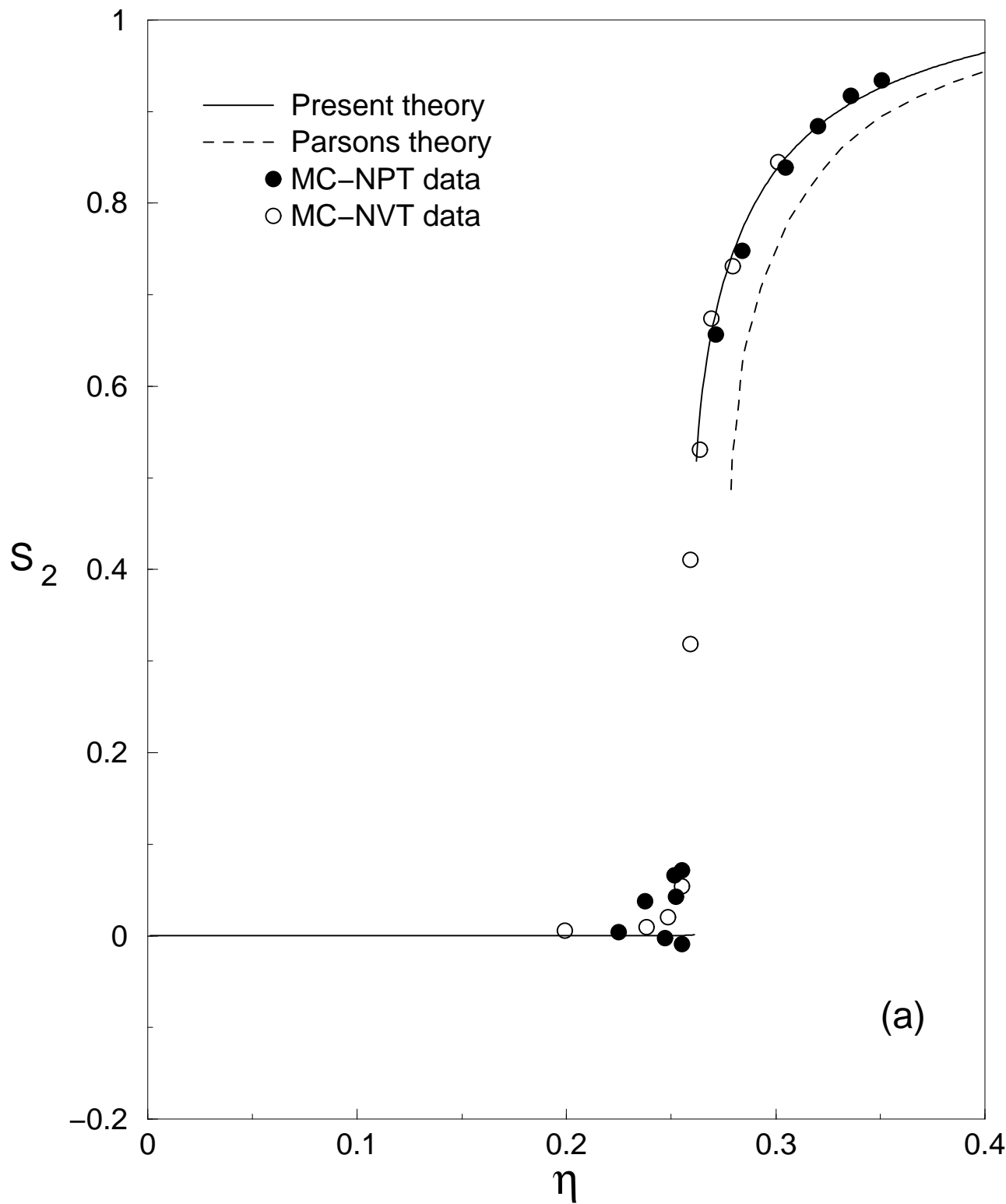


Figure 1(b). K.M. Jaffer: J. Chem. Phys.

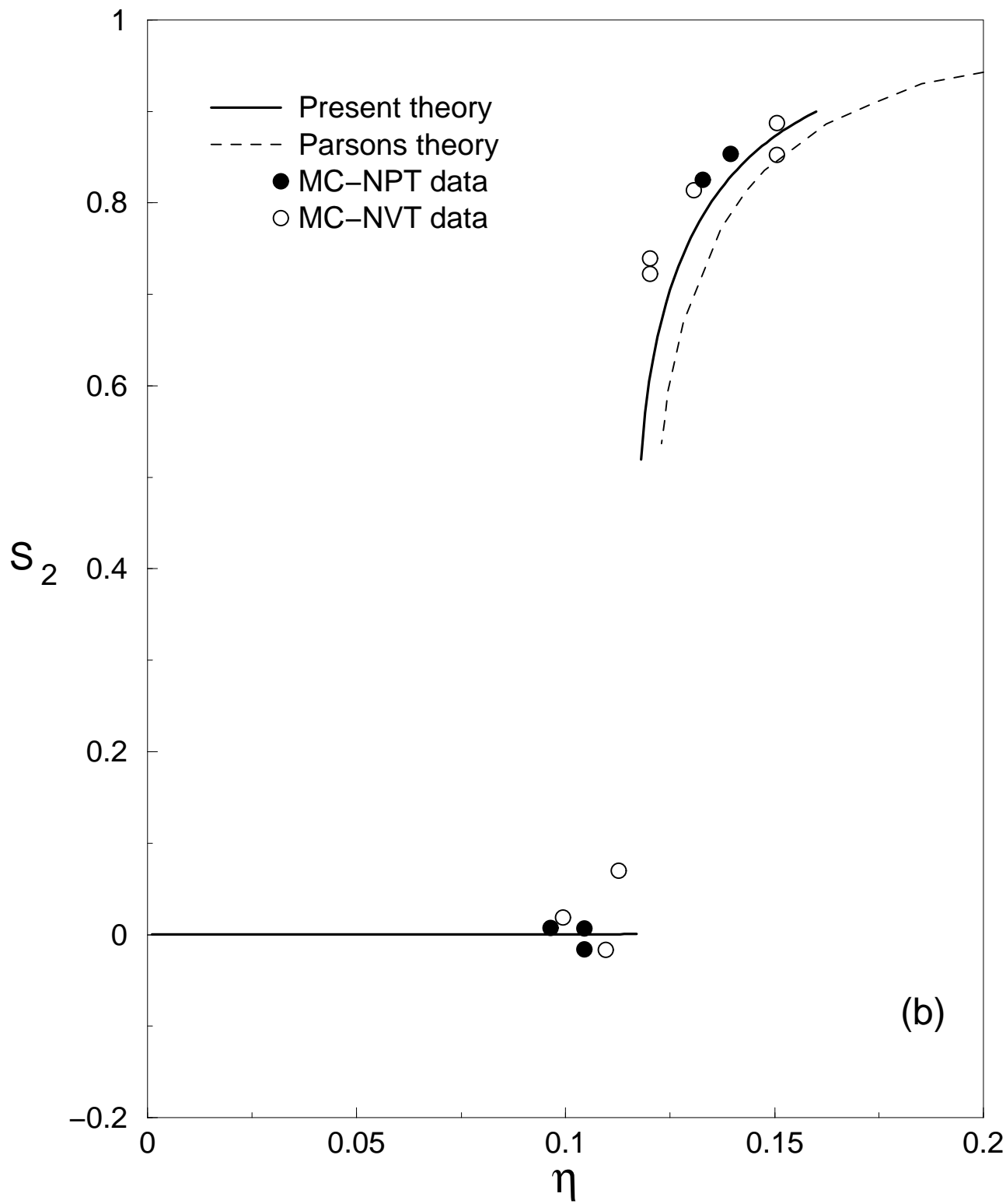


Figure 2(a). K.M. Jaffer: J. Chem. Phys.

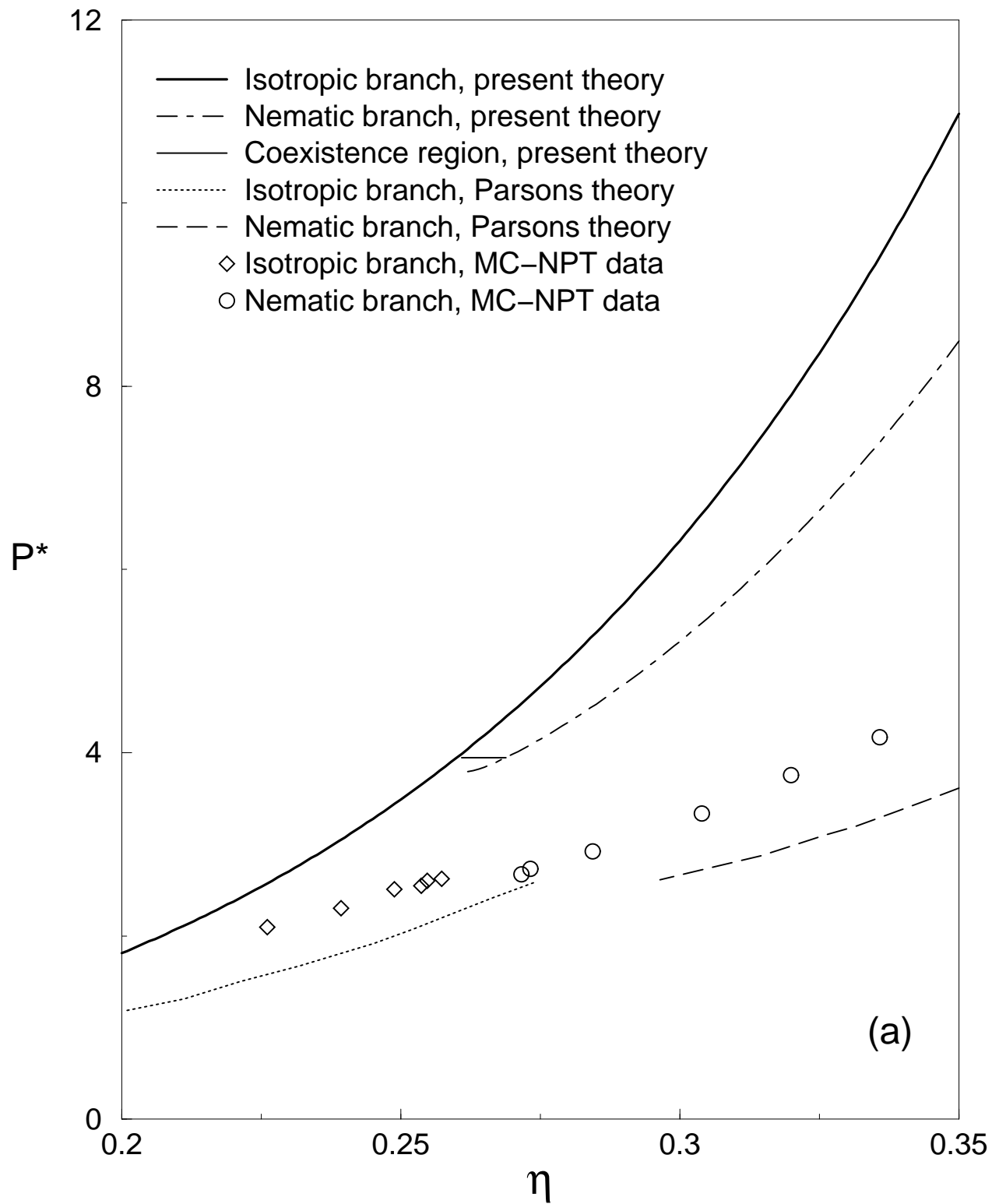


Figure 2(b). K.M. Jaffer: J. Chem. Phys.

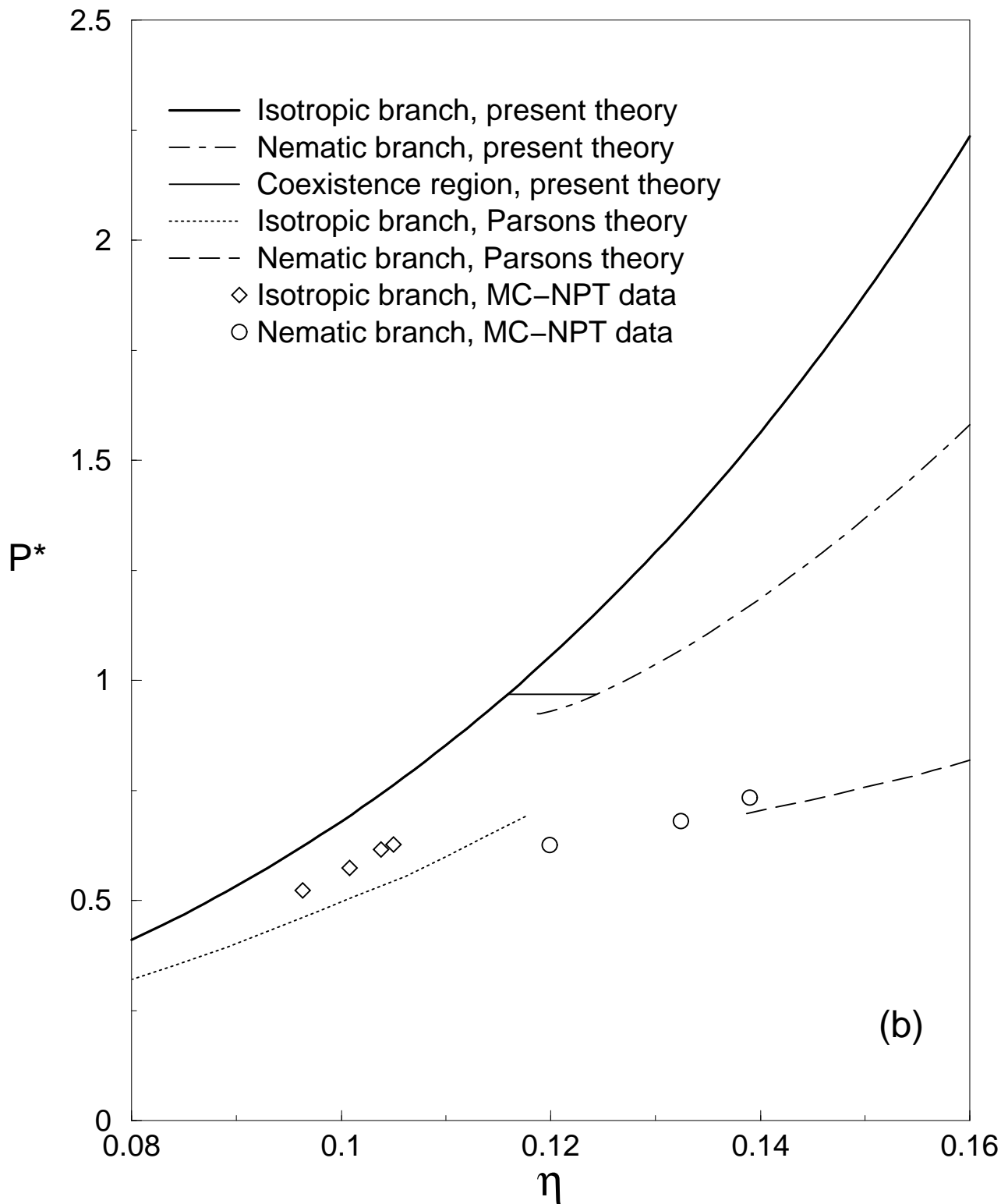


Figure 3. K.M. Jaffer: J. Chem. Phys.

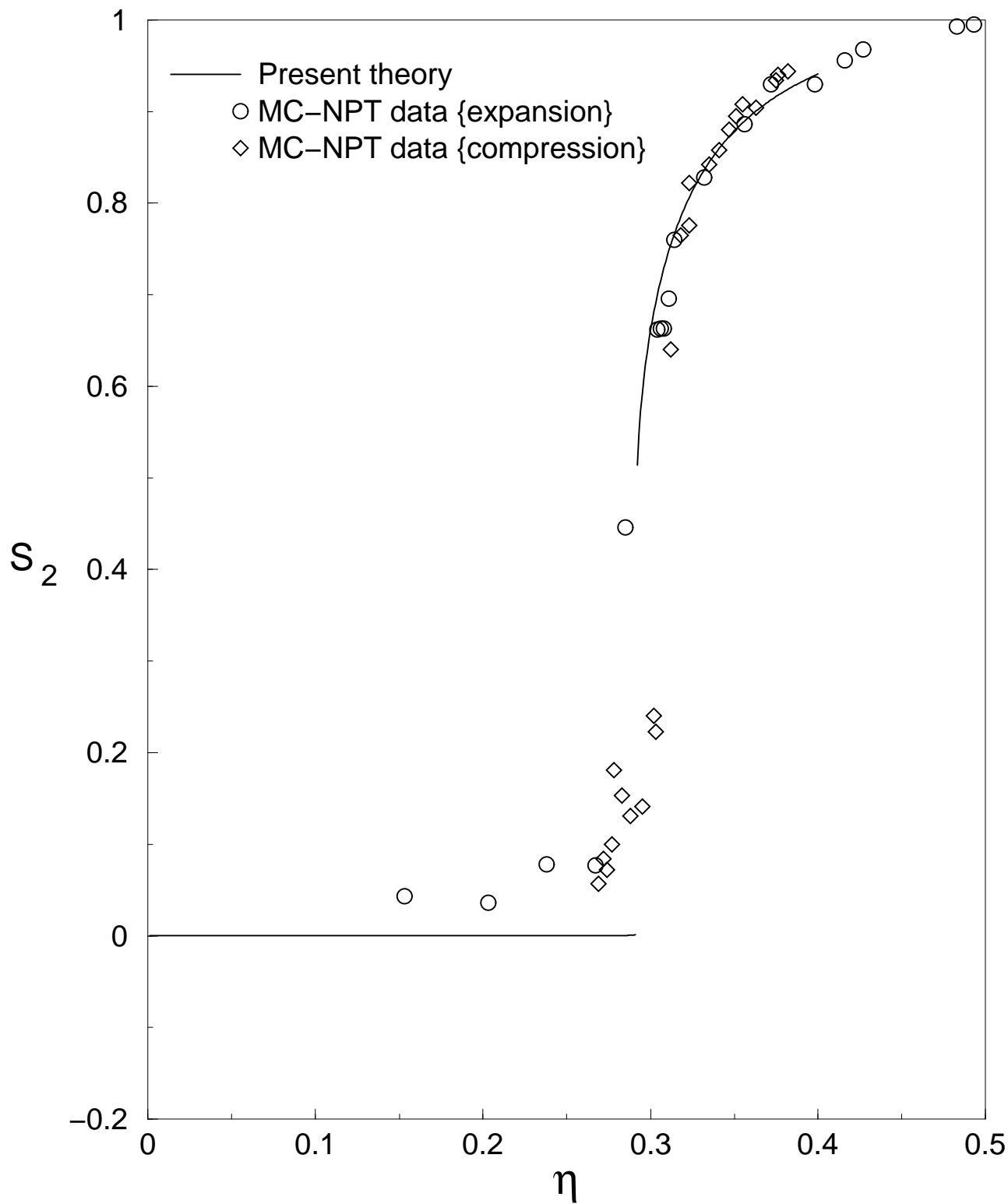


Figure 4. K.M. Jaffer: J. Chem. Phys.

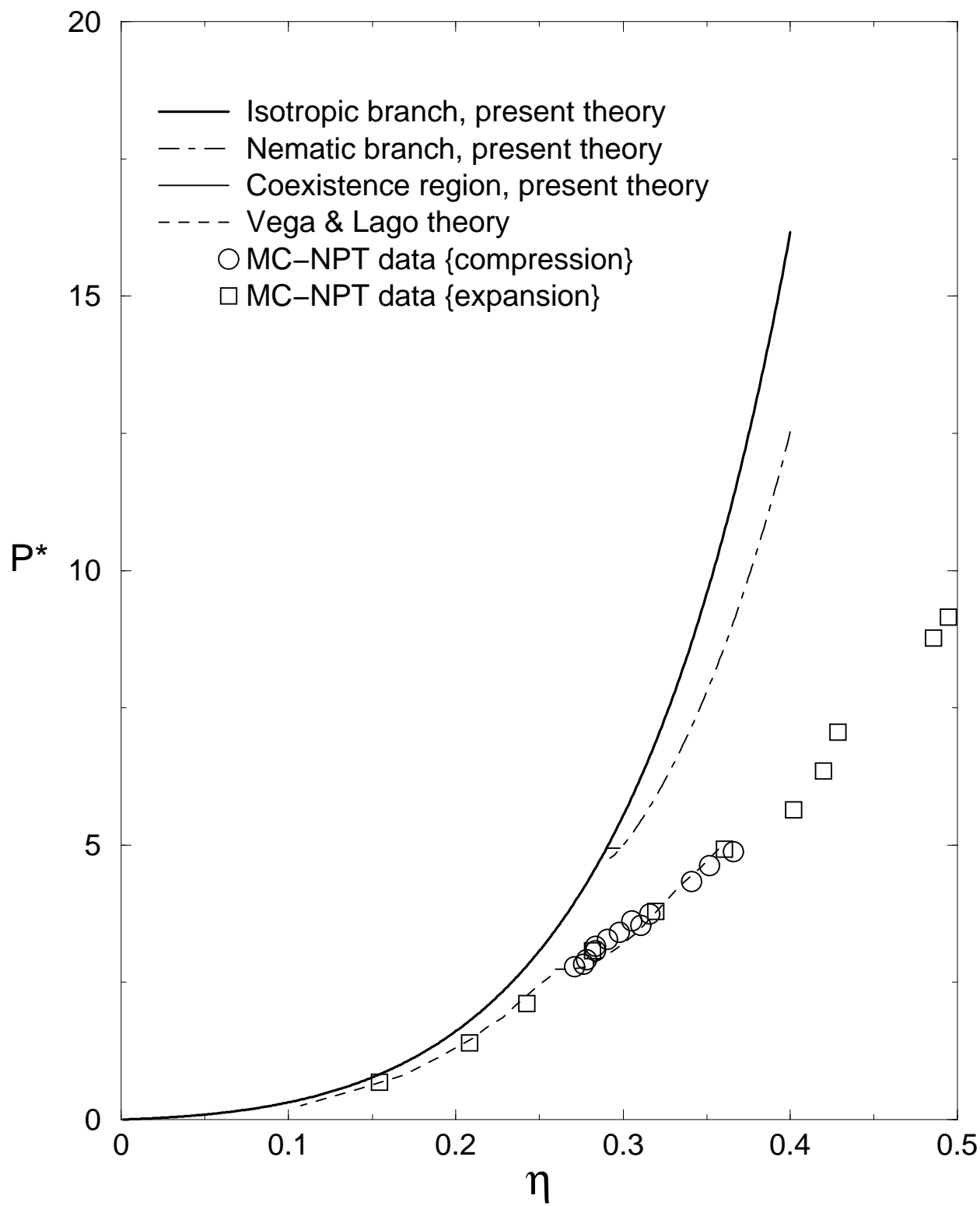


Figure 5. K.M. Jaffer: J. Chem. Phys.

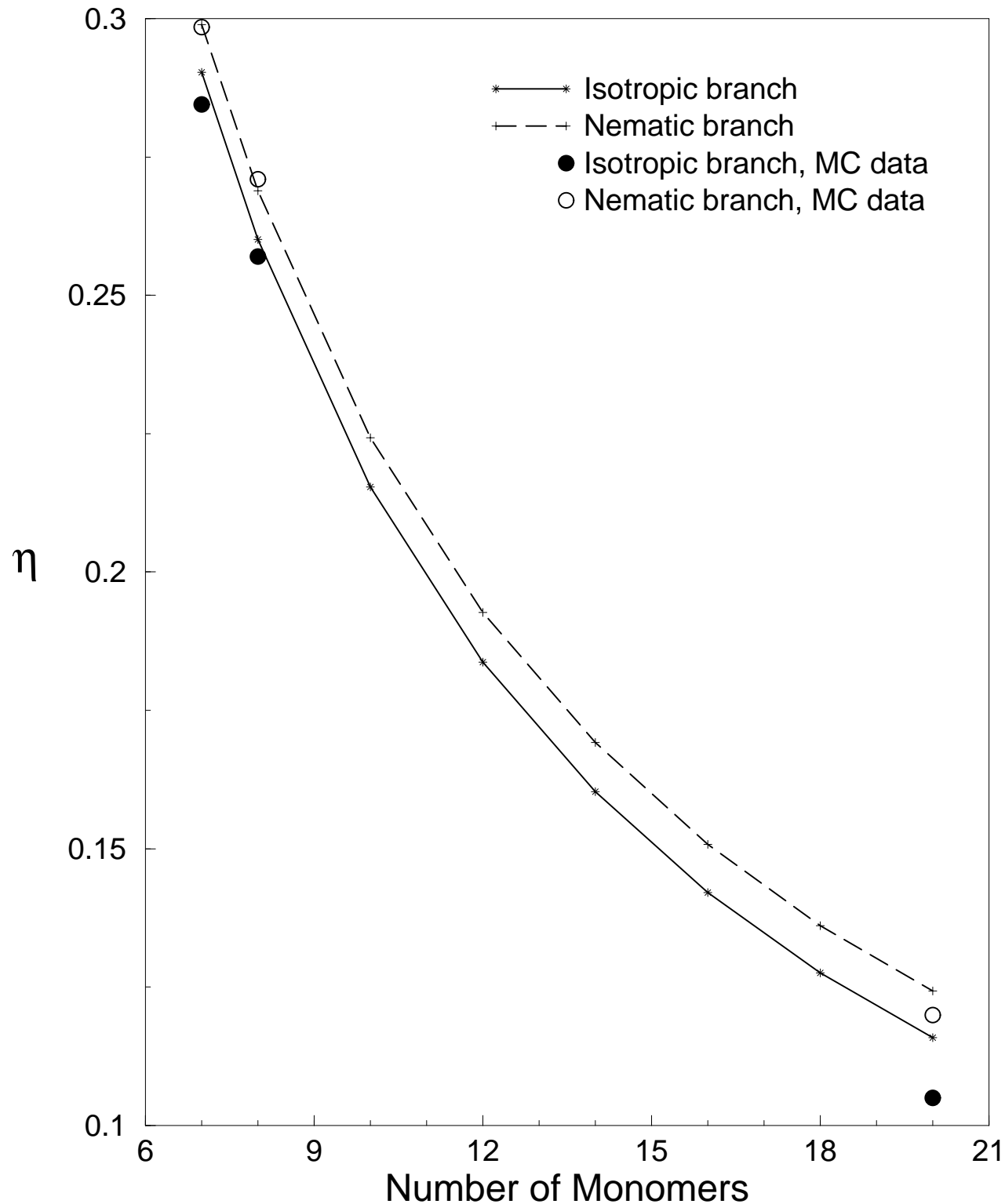


Figure 6(a). K.M. Jaffer: J. Chem. Phys.

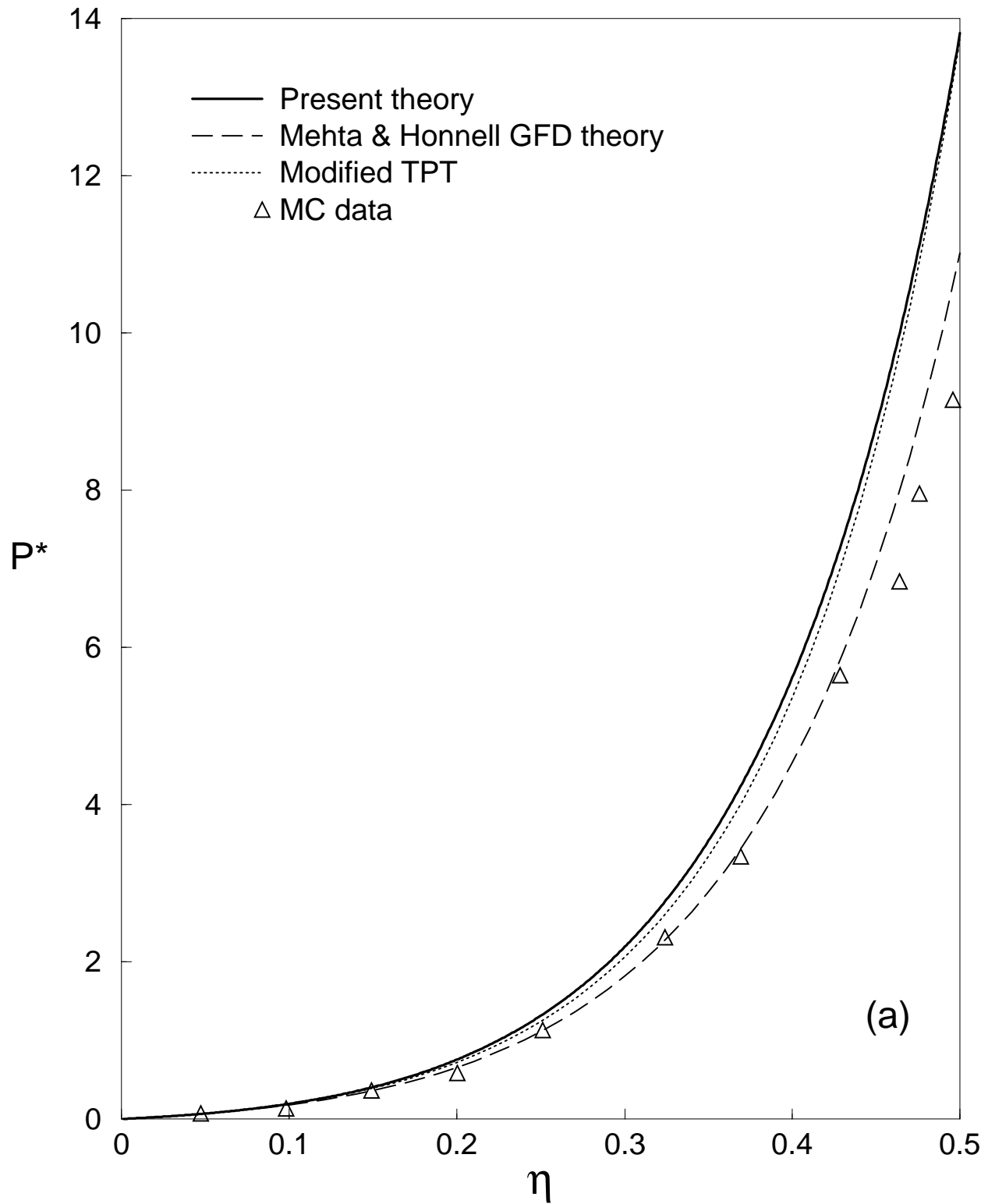


Figure 6(b). K.M. Jaffer: J. Chem. Phys.

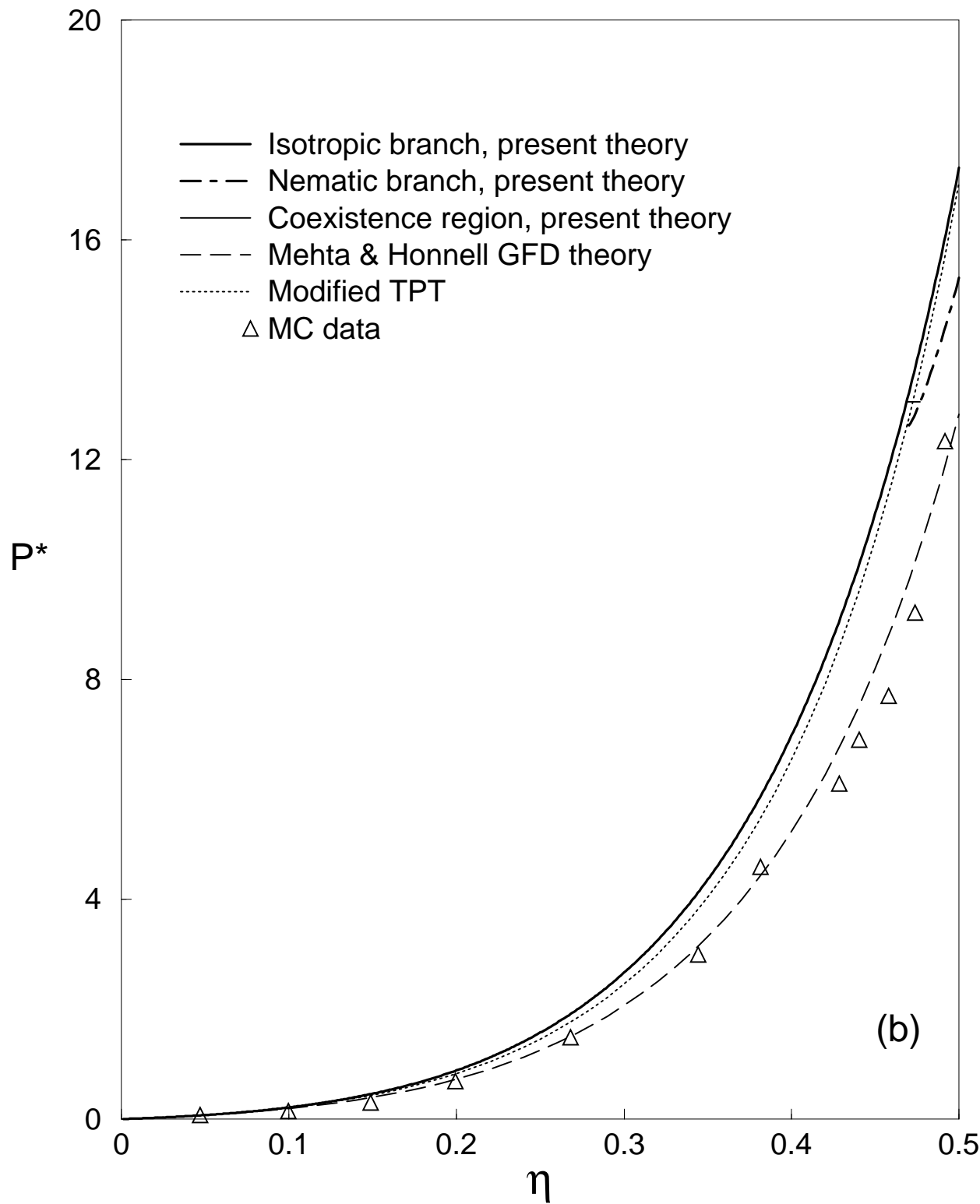


Figure 6(c). K.M. Jaffer: J. Chem. Phys.

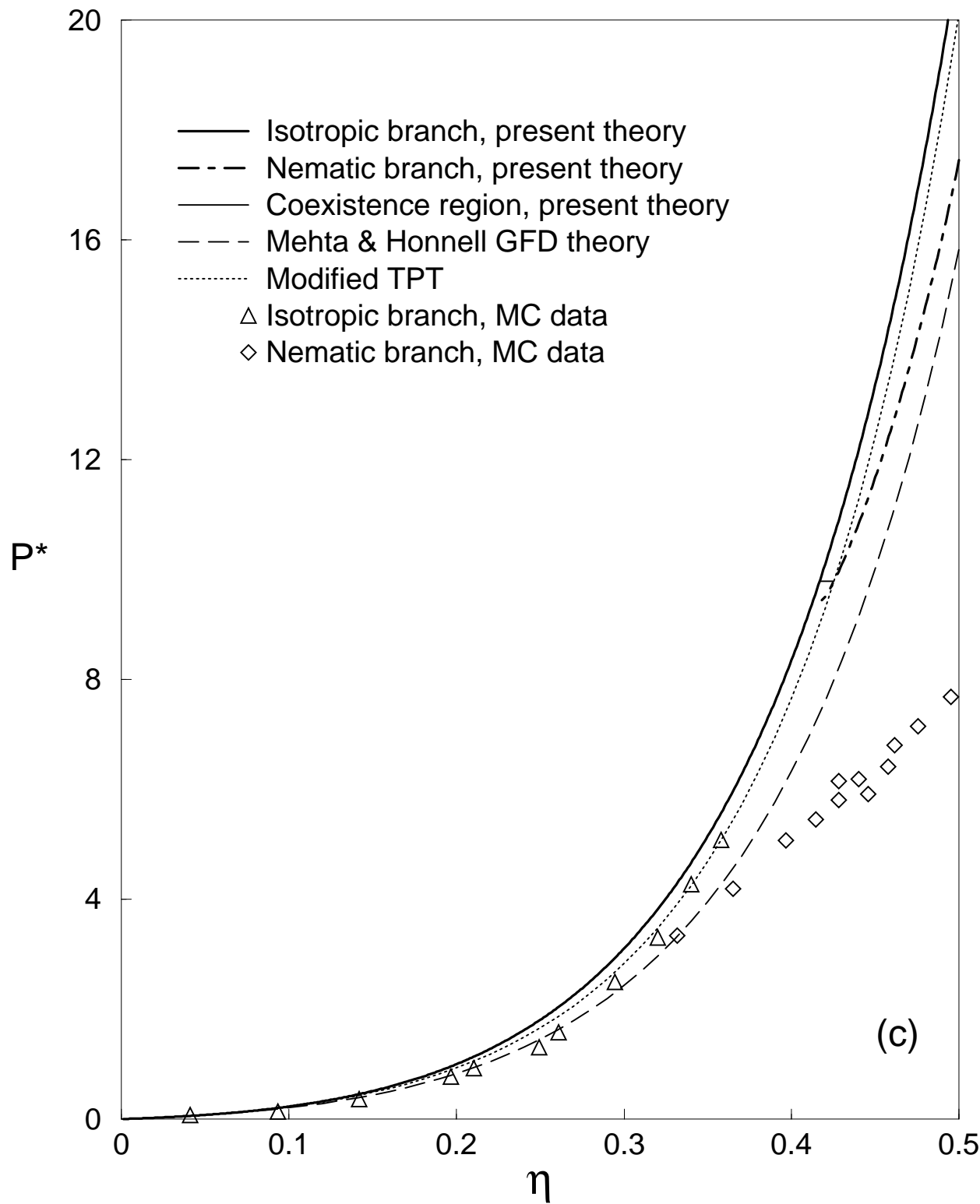


Figure 7. K.M. Jaffer: J. Chem. Phys.

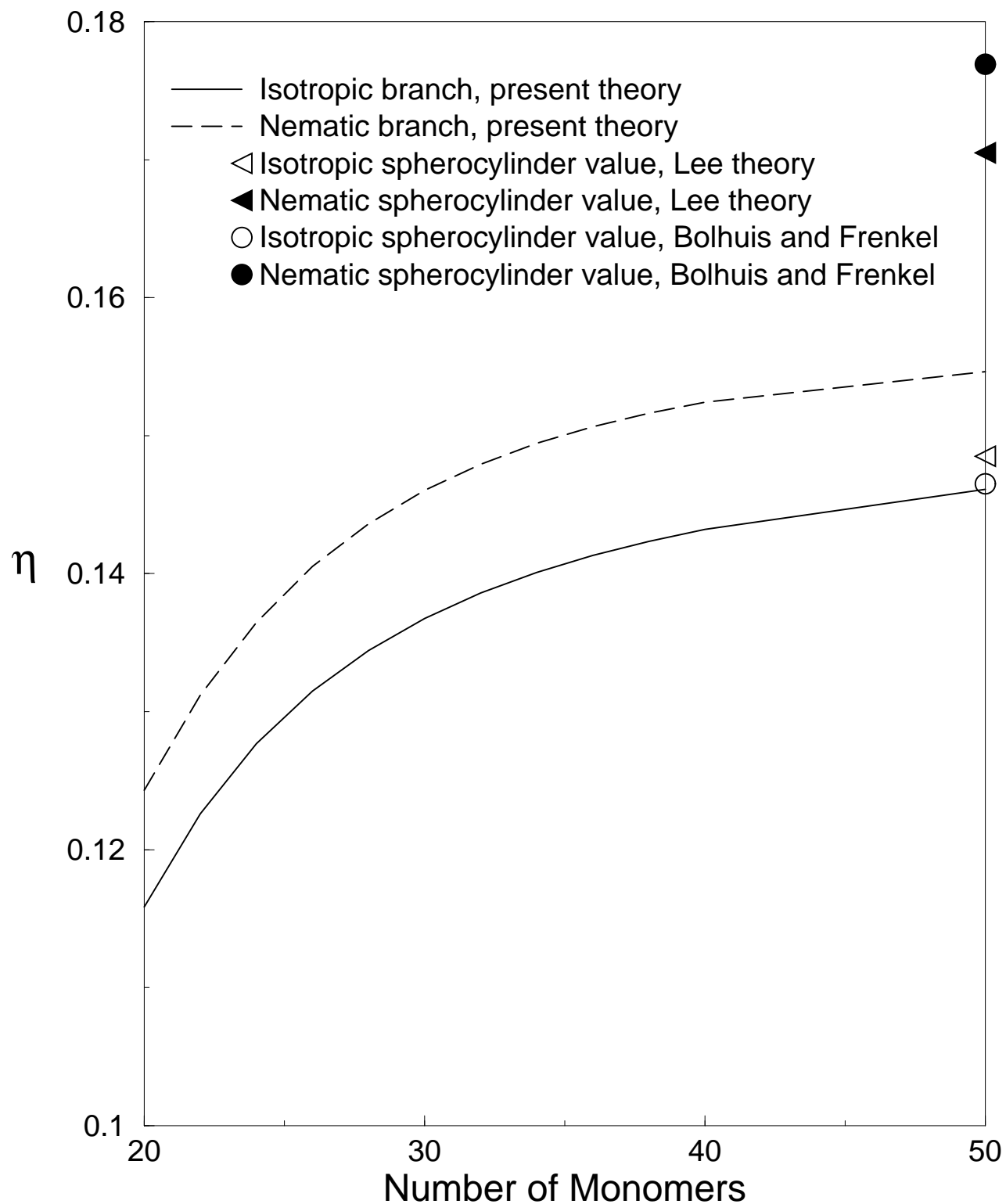


Figure 8. K.M. Jaffer: J. Chem. Phys.

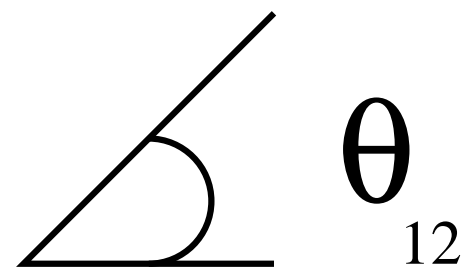
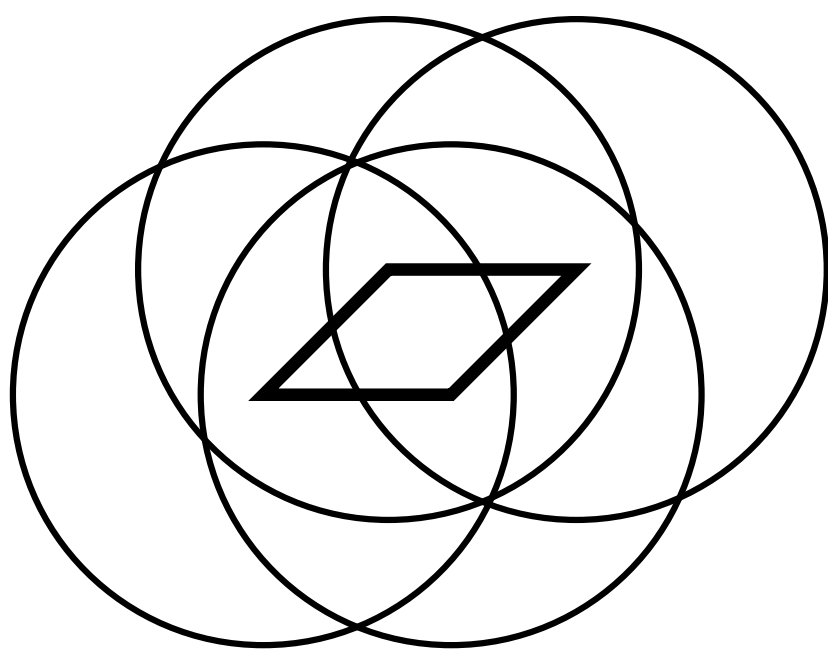


Figure 9. K.M. Jaffer: J. Chem. Phys.

